

C.1.
THE $^{12}\text{C}(p,\gamma)^{13}\text{N}$ REACTION

by

David Berghofer

S.B. M.I.T., 1971

A THESIS SUBMITTED IN PARTIAL FULLFILMENT OF
THE REQUIREMENTS FOR THE DEGREE OF
MASTER OF SCIENCE

in the Department
of
Physics

We accept this thesis as conforming to the
required standard:

In presenting this thesis in partial fulfilment of the requirements for an advanced degree at the University of British Columbia, I agree that the Library shall make it freely available for reference and study. I further agree that permission for extensive copying of this thesis for scholarly purposes may be granted by the Head of my Department or by his representatives. It is understood that copying or publication of this thesis for financial gain shall not be allowed without my written permission.

Department of Physics

The University of British Columbia
Vancouver 8, Canada

Date April 10, 1974

abstract

The ninety degree yield curve for the $^{12}\text{C}(p,\gamma)^{13}\text{N}$ reaction was examined for proton energies (E_p) between 14 MeV and 24.4 MeV using a 99.9 % pure carbon-12 target and protons from the University of Washington FN tandem Van de Graaff. The giant dipole resonance (GDR) for the gamma transition to the ground state (γ_0) was found to be centered at $E_p = 20.5$ MeV with a width $\Gamma = 4$ MeV and a maximum cross-section = 3 $\mu\text{b}/\text{sr}$. Intermediate structure of width $\Gamma = 1$ MeV was observed at $E_p = 17.5$ MeV and 23 MeV. The yield curve was compared to the $^{11}\text{B}(p,\gamma_0)^{12}\text{C}$ yield curve, and the similarities found indicated that valence nucleon transitions to the ground state play little part in the GDR of ^{13}N .

Yield curves for the transition to the first excited state (γ_1) and the sum of the transitions to the second and third excited states (γ_{2+3}) are also given in the regions where they can be reliably extracted. No fine structure was observed. Measured yields of the 12.71 MeV and 15.11 MeV gamma-rays from the inelastic reaction agree well with other recent results. Proton decay widths to these states from compound nuclear states in ^{13}N are given.

Angular distributions for the (p,γ_0) reaction were measured at six energies in the region of the "pygmy resonance", $E_p = 10$ MeV to 14 MeV, to inspect previously reported fine structure. Two narrow minima seen in the ninety degree yield are found to be minima in the integrated cross-sections, whereas the shape of the angular distribution is relatively constant.

The $^{12}\text{C}(p,\gamma)^{13}\text{N}$ Reaction

table of contents:		page
I	Introduction	
	A General	1
	B The Dipole Resonance in Mass-13 α Nuclei	5
II	Experimental Equipment and Procedure	
	A General Set-up	9
	B Gamma-ray Spectrometer	11
III	The $^{12}\text{C}(p,\gamma)^{13}\text{N}$ Reaction	
	A Yield and Angular Distributions in the Region of the Giant Resonance	18
	B Angular Distributions in the Region of the Pygmy Resonance	32
IV	Yields of the 12.71 MeV and 15.11 MeV Gamma-rays from the Inelastic Reaction $^{12}\text{C}(p,p'\gamma)$	41
	A Yield of the 15.11 MeV Gamma-ray	44
	B Yield of the 12.71 MeV Gamma-ray	51
	C Angular Distributions of the 12.71 MeV and 15.11 MeV Gamma-rays	55

V	Discussion	59
VI	Summary and Conclusions	70
	Appendix	72
	Bibliography	83

list of tables:	page
I Angular Distributions for protons scattered inelastically to the 15.11 MeV state in ^{12}C	24
II Calculated gamma-ray angular distributions for the $^{12}\text{C}(p,\gamma_0)$ reaction	37
III Decay widths of the 12.71 MeV and 15.11 MeV gamma-rays	42
IV Resonances in ^{13}N found in the yield of the 12.71 MeV and 15.11 MeV gamma-rays	47
V Angular distributions for 1^+ to 0^+ gamma-rays for the reaction $^{12}\text{C}(p,p'\gamma)$ where the intermediate radiation is unobserved	56

list of figures:	page
1 NaI crystal spectrometer	12
2 Schematic of the electronics	13
3 Efficiency and attenuation corrections	16
4 Typical spectrum	19
5 $^{12}\text{C}(p,\gamma_0)^{13}\text{N}$ gamma-ray yield	22
6 Angular distributions at 22.4 MeV and 23.3 MeV	27
7 $^{12}\text{C}(p,\gamma_1)^{13}\text{N}$ gamma-ray yield	29
8 $^{12}\text{C}(p,\gamma_{2+3})^{13}\text{N}$ gamma-ray yield	30
9 $^{12}\text{C}(p,\gamma_0)^{13}\text{N}$ gamma-ray yield in the region of the pygmy resonance	33
10 γ_0 angular distributions in the region of the pygmy resonance	34
11 γ_0 angular distribution Legendre polynomial coefficients	36
12 15.11 MeV and 12.71 MeV gamma-ray yields	45
13 Legendre polynomial coefficient for the 15.11 MeV gamma-ray	58
14 $^{12}\text{C}(p,\gamma_0)^{13}\text{N}$ gamma-ray yield from 2.8 MeV to 24.4 MeV	60
15 $^{13}\text{N}(\gamma,p)$ and $^{13}\text{C}(\gamma,x)$ cross-sections	63
16 $^{11}\text{B}(p,\gamma_0)$ and $^{12}\text{C}(p,\gamma_0)$ cross-sections	66
17 Geometric model for double solutions to interfering Breit-Wigner resonance shapes	79

acknowledgment

I would like to thank Drs. Measday, Hasinoff and Mulligan for their very patient explanations to a novice in the field. The experiment would not have been completed without the help of the other graduate students in the group: B. Lim, J. Spuller, and K. Ebisawa. I would also like to thank my wife, Marta, for some excellent lettering and a great deal of understanding.

I INTRODUCTION

A General

The giant dipole resonance (GDR), the broad peak seen in photo-nuclear cross-sections, is a phenomenon observed in essentially all nuclei. Many variations on the two basic models, the collective model and the independent particle model, have been used to describe the absorption process. Both models have been quite successful in describing most features of the giant resonance. This would seem to indicate that the two models are not as different as they at first appear, and indeed Brink, 1957¹, has shown that, in some sense, the models are equivalent.

The collective model, first proposed by Goldhaber and Teller, 1948,² pictures dipole photo-absorption as producing a collective motion whereby all the protons in the nucleus oscillate against all the neutrons in the nucleus. This is essentially a quantized hydro-dynamic model, whereby a proton "fluid" and a neutron "fluid" vibrate against each other. This collective model postulates ad-hoc collective variables, such as density and velocity distributions, in the "continuous" nuclear medium, rather than dealing with the dynamical variables of the individual nucleons.

The energy of the giant resonance varies from 23 MeV for light nuclei to 14 MeV for heavy nuclei, and its width varies from 3 MeV to 8 MeV. In the collective model, the resonant

energy is a function of nuclear radius, and the width of the resonance arises from friction experienced by the interpenetrating fluids. The radius and other collective parameters can be determined from the low-energy spectra (i.e. the moment of inertia of the nucleus can be determined from transitions between low lying rotational states). The friction term cannot, at present, be calculated from the microscopic model, and must be taken from phenomenological systematics. Thus, giant resonance shapes and strengths can be calculated with no free parameters and, for those heavy nuclei where the calculation has been carried out, reproduce experimental results quite well.³ In addition, the collective model readily explains the splitting of the giant resonance into two peaks for deformed nuclei. For these nuclei, the collective model indicates two primary modes of vibration-- a low frequency mode along the long symmetry axis, and a high frequency mode along the short axis. The two frequencies correspond to the energies at which the cross-section peaks. This splitting is very apparent in such deformed nuclei as holmium.⁴ Recent developments of the collective model include a three fluid picture, where the excess neutrons are treated as a separate entity.³

The collective model smooths over nuclear structure into fluids by averaging the collective motion of many nucleons, and so, should be more applicable to heavy nuclei ($A > 40$) than to light nuclei.

The independent particle model (IPM) of the GDR is based on the shell model, and was first developed by Wilkinson, 1956⁵. Since the ground states of nuclei are well described by the shell model, the IPM pictures photo-absorption as exciting a single nucleon to a more energetic orbital shell. The width of the giant resonance cannot be accounted for as the broadening of a single-particle single-hole (lp-lh) state, although calculations with a finite potential well do show some broadening. Instead, the giant resonance is often viewed as a coherent mixture of many lp-lh states.

First estimates of the energy of the GDR using the IPM were significantly below experimental values. Attempts were made to remove the discrepancy by introducing non-local or velocity dependent forces, with little success. The discrepancy was successfully removed by including a repulsive particle-hole interaction. This is simply another way of describing the attraction to the nucleons in an unclosed shell experienced by an excited nucleon. This "repulsion" increases the calculated energy of the GDR. As Brink has shown¹, this interaction is a many body correlation which produces a collective motion of neutrons against protons, i.e. the collective model. Theoretical estimates of the energy now agree well with experimental values.⁴

Intermediate structure in the giant resonance, which is seen in many nuclei (e.g. ^{16}O and ^{28}Si) is viewed according to the IPM as well-defined shell-model configurations (not necessarily lp-lh states). In some cases, such a well-defined configuration

in the giant resonance can be identified by the variation in the angular distribution of the photo-nucleons (or of the gamma-rays in the inverse reaction). This, however, points out a major difficulty of the IPM of the giant resonance. Angular distributions throughout the resonance, for the most part, vary little, if at all. This contradicts the notion of many lp-lh states acting coherently, as has been noted by Allas, et. al.,⁶ 1964, and Tanner,⁷ 1965. As Tanner's analysis indicates, the GDR should probably be regarded as a single broad resonance, and thus, the IPM cannot easily account for its width. Still, mixtures of single particle wavefunctions are frequently used to describe the GDR in many theoretical calculations.

An important variation on these two models is the schematic model of Brown and Bolsterli.⁸ This model is again based on the mixing of lp-lh excitations by the particle-hole interaction. By making some radical simplifying assumptions, Brown and Bolsterli show that the coherent effect of the many states can push a single eigenstate to an energy much higher than the single-particle excitation energies, and at the same time, endow this state with essentially all of the dipole transition strength. This model is simple and elegant, and gives some insight into the more detailed particle-hole calculations, but yields realistic quantitative predictions only with great difficulty.

B The Dipole Resonance in Mass-13 Nuclei

The mass-13 nuclei ^{13}C and ^{13}N have a very simple structure: a valence nucleon added to a carbon-12 core. If the additional nucleon does not cause a major disturbance in the core, the carbon-12 will remain in its ground state, a closed subshell. Carbon-12 is a light $4n$ nucleus. The GDR in carbon-12 comes at an excitation energy $E_x = 23$ MeV. This concentration of strength at a high energy is ascribed to the mechanism of the schematic model, which seems to well describe $4n$ nuclei, with especially symmetric spatial wave-functions. Recent results indicate the overall structure of the GDR in ^{12}C can be mostly derived from semi-phenomenological $1p-1h$ wave-functions.⁹

Mass-13 nuclei are among the simplest non-closed shell nuclei. Their study should yield some insight into the structure of non-closed shell nuclei in general, and in particular, into how a closed shell nucleus is affected by the addition of a single nucleon.

The nuclei ^{13}C and ^{13}N have been well-studied, and many levels have been documented.¹⁰ However, the study of the GDR, and in particular, the single nucleon decay of the dipole resonance, has not been exhaustive. Carbon-13 is a stable isotope, and can thus be studied directly. The reactions $^{13}\text{C}(\gamma, p)^{12}\text{B}$ and $^{13}\text{C}(\gamma, n)^{12}\text{C}$ have been examined from photon energies (E_γ) between 5 MeV and 38 MeV by Cook in 1957,¹¹ and this remains the most complete study to date.

Nitrogen-13 is an unstable isotope, β^+ decaying to carbon-13 with a lifetime of about ten minutes. The present work is an examination of the dipole resonance in ^{13}N by means of the inverse radiative proton capture reaction: $^{12}\text{C}(p,\gamma_0)^{13}\text{N}$. This reaction is related to the reaction $^{13}\text{N}(\gamma,p_0)^{12}\text{C}$ by the principle of detailed balance.¹² (A subscript 0,1... on the p and γ indicates transitions leaving the residual nucleus in the ground state, first excited state, etc.) In this case, the principle of detailed balance is valid even if time reversal invariance is violated.¹³ While the proton transition to the ground state in general represents the structure of the GDR fairly well, distortions do occur.¹⁴ In particular, this mode of decay may be quite important at low energies, but may become less important at higher energies, where more decay channels are energetically allowed. Thus, the (γ,p_0) cross-sections do not necessarily reflect the gross shape of the GDR. Some care must also be taken when interpreting structure in radiative capture reactions. Tanner points out that such structure may be the result of weak compound nuclear states interfering with the main broad resonance, and thus, not really representative of the GDR.⁷ However, even with these uncertainties, radiative capture has proved a powerful tool for studying the GDR.

Until recently, the $^{12}\text{C}(p,\gamma)^{13}\text{N}$ capture reaction has been rather neglected. Warburton and Funsten were the first to detect the capture gamma-ray γ_0 in 1962.¹⁵ In 1963, Fisher, et al. examined the reaction over a wider range.¹⁶ Both experiments

were limited by the poor energy resolution of both the proton beams (300 keV and 800 keV respectively) and the small NaI detectors ($\approx 13\%$). A more recent study by Dietrich was limited to a small region about the lowest $T = 3/2$ state in ^{13}N .¹⁷ Recent work on the capture reaction has been done at the University of Washington in Seattle. Johnson has examined the reaction from 2.8 MeV to 9 MeV.¹⁸ Measday, Hasinoff and Johnson have examined the capture reaction from 9 MeV to 16 MeV.¹⁹ The present report extends this study to 24.4 MeV.

The GDR in ^{13}N can also proton-decay to the ground state or excited states of ^{12}C . Thus, the proton and gamma-ray cross-sections from the $^{12}\text{C}(p,p)$ and $^{12}\text{C}(p,p'\gamma)$ elastic and inelastic reactions might also contain information about the GDR in ^{13}N . In the present study, we also examine the yields of the 12.71 MeV and 15.11 MeV gamma-rays excited in the inelastic reaction. Proton yields from the elastic and inelastic reactions for incident proton energies between 9.4 MeV and 21.5 MeV have been measured by Levine and Parker,²⁰ who also measured the $^{12}\text{C}(p,\alpha)$ decay. Data with a polarized proton beam have been taken by Meyer and Plattner.²¹ The neutron decay channel in ^{13}N has been studied via the $^{12}\text{C}(p,n)^{12}\text{N}$ reaction by detecting positrons from decay of the ground state of ^{12}N by Rimmer and Fisher.²²

The results of Fisher, et. al.,¹⁶ showed a peak at a proton energy $E_p = 13$ MeV, separated from the main resonance near $E_p = 20$ MeV. Our results confirm this. This lower peak has sometimes been called a "pygmy resonance". The term "pygmy resonance" has been applied several ways in nuclear physics. In neutron

capture spectroscopy, the term applies to broad peaks seen in certain mass regions. When referring to the GDR, "pygmy resonance" sometimes refers to that part of the dipole resonance with the lower allowed value of isospin ($T_{<}$)²⁴. For this report, the term "pygmy resonance" will refer only to that part of the dipole resonance at an energy significantly lower than the main strength of the resonance.

The present report also includes the measurement of six angular distributions in the region of the pygmy resonance, and two angular distributions at a higher energy. We shall attempt to view all the data in this report in light of the following questions:

- 1) To what extent does the valence nucleon disturb the ^{12}C core?
- 2) Do single-particle transitions involving the valence nucleon contribute significantly to the dipole resonance?
- 3) To what extent can we identify resonances seen in other reactions with the GDR?

II EXPERIMENTAL EQUIPMENT AND PROCEDURE

A General Set-Up

The ^{13}N nucleus has a single valence proton outside the closed shell configuration of ^{12}C . Thus, the proton binding energy for ^{13}N is 1.944 MeV (= Q value), a small number when compared with the proton binding energy of 15.957 MeV for ^{12}C . To study the full giant resonance region of ^{13}N by radiative proton capture, proton energies from 10 MeV to 30 MeV would be required. Present day Van de Graff accelerators, with a maximum of approximately 25 MeV, cover most, but not all, of this region. A study of the giant resonance through the inverse (p, γ) reaction has the advantage of exhibiting more fine structure than is possible when examining the direct (γ ,p) or (γ ,n) reactions, because the incident beam of charged particles possesses far better energy resolution than any beam of photons, at present. Also, the dipole resonance for unstable isotopes, in particular ^{13}N , which are inaccessible in the direct reaction, can be studied by the capture reaction. The University of Washington's FN tandem Van de Graff can routinely achieve an energy resolution of better than 5 keV for 15 MeV protons, an uncertainty even less than the energy loss in the target (\cong 10 keV).

In general, energy calibration was no problem for the $^{12}\text{C}(p,\gamma)$ spectra. For incident proton energies greater than $E_p = 17$ MeV, the 12.71 MeV and 15.11 MeV gamma-rays from the

inelastic reaction were plainly visible, thus fixing the energy calibration). When below these thresholds, an energy calibration was done for low-energy gamma-rays from radioactive sources, and the gain was then decreased by a known amount, to bring the capture gamma-rays within the energy range of the analyzer.

The signals from the spectrometer were analyzed by a pulse height analyzer (PHA) and sorted into ACCEPT and REJECT bins, as discussed in the following section. At the end of a run, the data were dumped into an SDS computer and then stored on magnetic tape for later analysis. A version of the EGG program (see appendix) had been adapted for use on the SDS computer, allowing an immediate on-line analysis while the data was being taken. This is a great aid to the experimenter, permitting him to further investigate interesting results at once. Final analysis of all data was done on a time-sharing IBM computer at the University of British Columbia.

B The Gamma-Ray Spectrometer

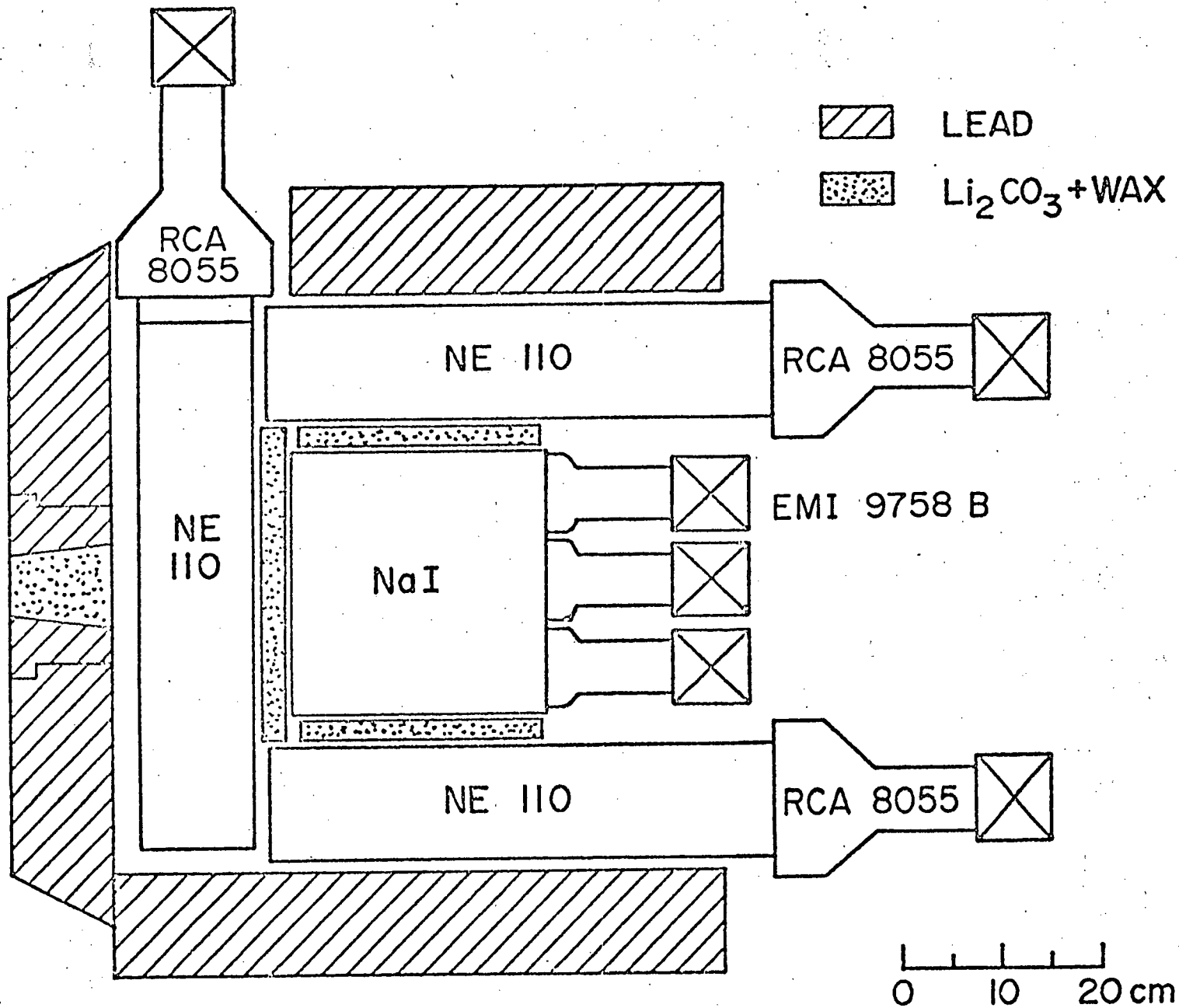
The gamma-ray detector used in this study belonged to a University of British Columbia group, but resided at the University of Washington Nuclear Physics Laboratory. A detailed description of the spectrometer has been published (Hasinoff et al., 1973²⁵), only a brief account will be given here.

The design of the spectrometer and housing is illustrated in figure 1, page 12 . The central NaI(Tl) crystal, a cylinder 25.4 cm. in diameter by 25.4 cm. long, was manufactured by the French company Quartz et Silice. The response of the crystal to a 1.33 MeV gamma-ray from a collimated source moved along its axis was uniform to +0.75 %. A 1 cm. thickness of lithium carbonate and wax surrounds the sides and front face of the crystal, and provides some absorption of slow neutrons. The anti-coincidence shield consists of NE 110 plastic scintillator, 10.8 cm. thick.

A schematic of the electronics is shown in figure 2, page 13 . A complete description of the electronics is given by Lim, 1974.²⁶ Note that the anode signal is used for both the linear signal and the timing. This was found to be simpler than using the dynode signal for the linear pulse, and caused no loss of resolution.

A gain-stabilizing unit was attached to the power supply of the crystal's photo-tubes, because the gain of the photo-tubes

Figure 1



Na I

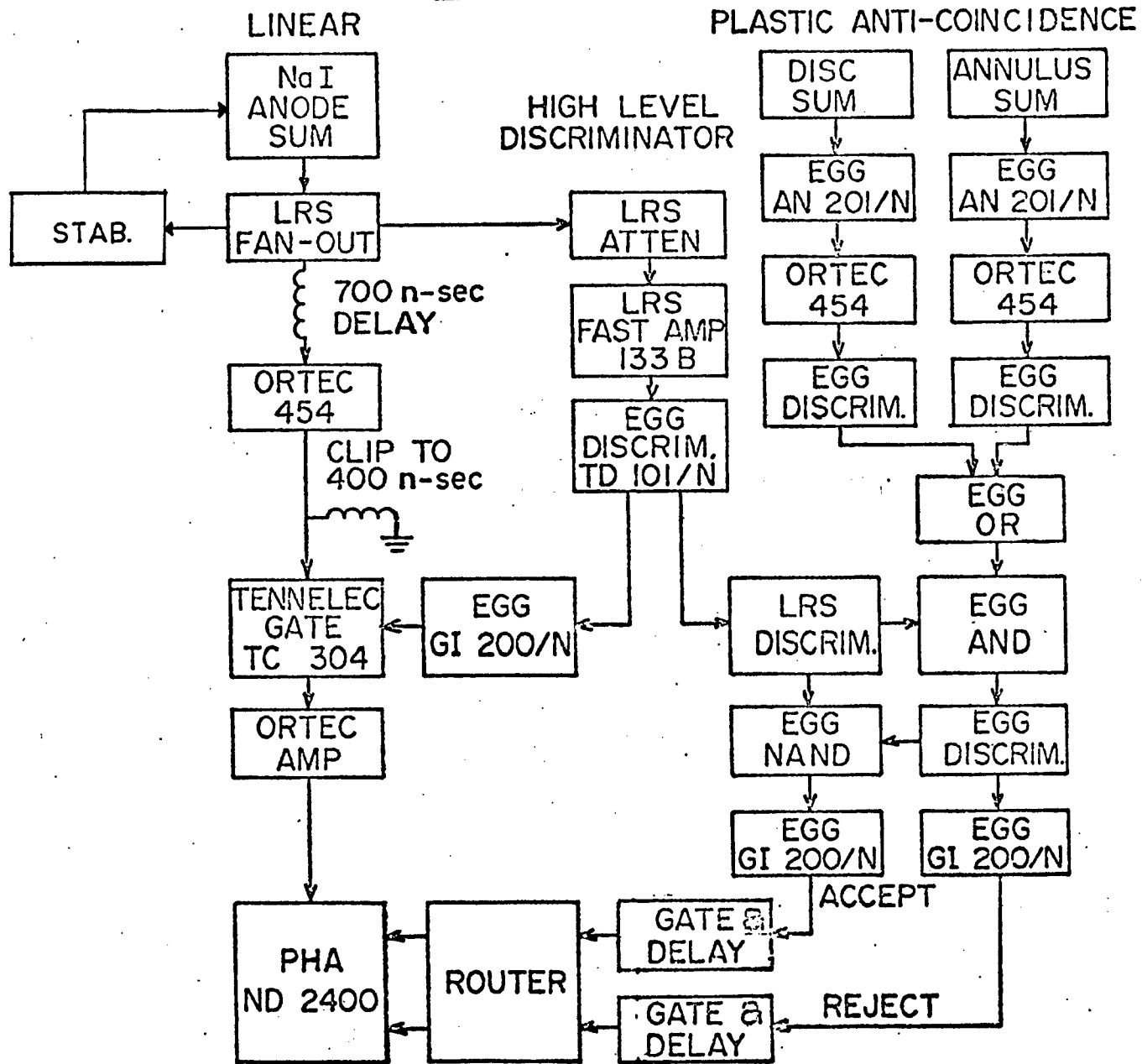


Figure 2

was a non-linear function of the counting rate. With the stabilizing unit, the gain shift was decreased to about 1 %, which caused no difficulty in identification of the lines. The stabilizer window was usually set on the 4.43 MeV gamma-ray from the first excited state of ^{12}C .

Cosmic ray rejection using the anti-coincidence shield can be made better than 200 to 1. This spectrometer has achieved a resolution of 3 % FWHM for 15 MeV gamma rays, using a collimator of solid angle 0.035 sr. The yield curve in this report was taken with a collimator of solid angle = 0.077 sr., half-angle = 7° . This gave a resolution (FWHM) = 4 %, which was more than adequate. For the angular distributions, the crystal was moved back to maximize the range of angles. The data was taken with no collimator, corresponding to approximately the same solid angle, causing the energy resolution to worsen slightly, to FWHM = 4.5 %. The detector could be moved between about 42° and 140° .

The angular alignment of the crystal was checked mechanically before each run. Recently, other members of the lab have tested the alignment by placing a radioactive point source in the target holder. The measured yield was isotropic to within 5 %.

Most of the data for the yield curve were taken during a single run. For this run, paraffin was placed in front of the detector to reduce the neutron background. The paraffin also significantly attenuates the gamma-rays, as does the front plastic used in anti-coincidence.

The anti-coincidence shield, which significantly improves the resolution of the NaI crystal, causes some of the gamma-rays

to be "rejected". These gamma-rays are stored in a separate bin as the REJECT spectrum. When calculating the absolute yield from the ACCEPT spectrum, a correction for the percentage of gamma-rays rejected must be applied to the data, in addition to the various attenuation factors. The former correction, called the "electronic efficiency", is a function of the gain of the photo-tubes on the plastic scintillator, but also depends on the size of the collimator and on the energy of the gamma-ray itself. For the 10" by 10" NaI crystal, approximately 100 % of 15 MeV gamma-rays interact, i.e. deposit some energy. Thus, the electronic efficiency, defined by

$$\text{El. Eff.} = \frac{\# \text{ in ACCEPT}}{\# \text{ in ACCEPT} + \# \text{ in REJECT}}$$

for an isolated gamma-ray, need only be folded into the attenuation factors to give a total correction value.

A calculation of the correction factor for the experimental set-up used in this study has been done. The result is given in figure 3 on page 16 . The electronic efficiency is a smooth fit to three experimental data points. The paraffin attenuation curve is a theoretical calculation normalized to one data point. The front plastic curve is a purely theoretical calculation, derived using the plastic's thickness and chemical composition, and known mass absorption factors.²⁷ The total correction curve is seen to vary little as a function of gamma-ray energy. From $E_g = 14 \text{ MeV}$ to 25 MeV, this correction varies by less than 5 %.

EFFICIENCY AND ATTENUATION CORRECTIONS
FOR THE 10"X10" NaI CRYSTAL DETECTOR

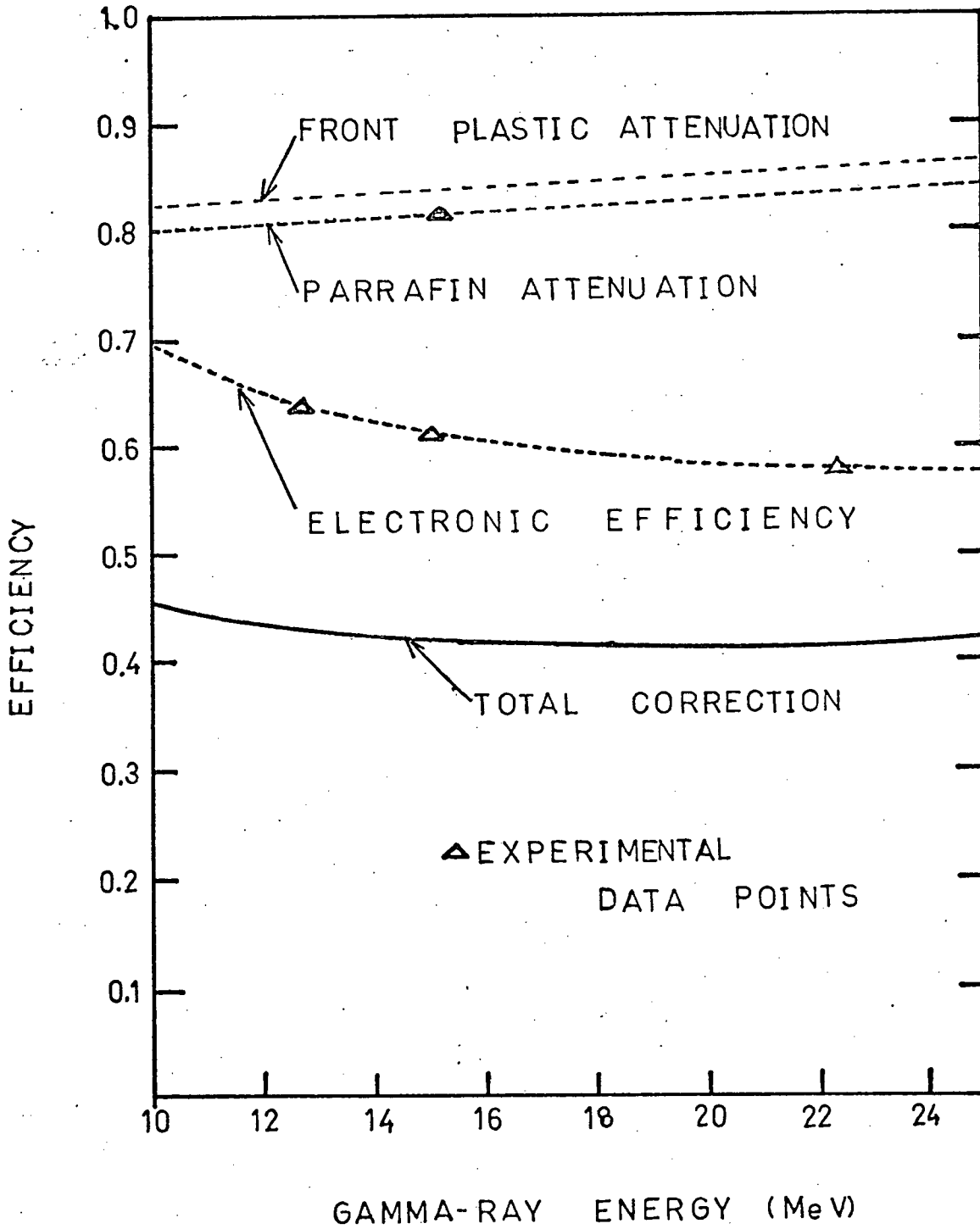


Figure 3

The absolute uncertainty of this curve is not more than 10 %. Since the variation with energy was small, a constant correction at 15.11 MeV, where it is better known experimentally, was uniformly applied to the data.

The data point for the electronic efficiency at 22.4 MeV was taken at a separate run. There was some discrepancy in the absolute normalization for different runs, and thus the electronic efficiency curve given is somewhat in question. For the worst possible case, the relative yield curves should be tilted, increasing the yield at 22 MeV by 10 %, and leaving the yield at 15.1 MeV unchanged. Further studies of the efficiency for this geometry are being made to remove the possible discrepancy.

A pure carbon-12 target (99.9% ^{12}C) was used throughout this study. The target thickness was measured using the narrow ($\Gamma = 1.3 \pm 0.3$ keV) $T = 3/2$ resonance in ^{13}N at proton energy $E_p = 14.231$ MeV. The target thickness was found to be $380 \mu\text{g}/\text{cm}^2 \pm 10$ %, in good agreement with previous measurements.

For spectrometers of this type, the behaviour of the gamma-ray line shape in the low energy tail region has not been determined. The present results have been analyzed by extrapolating the tail linearly to zero energy at zero counts. The alternative extreme, extrapolating the tail horizontally, would increase the stated yields by 12 % at $E_g = 24$ MeV and by 8 % at $E_g = 14$ MeV. Combining this with the uncertainties in target thickness and detector efficiency, we estimate an uncertainty of ± 30 % in our absolute cross-section normalizations.

III THE $^{12}\text{C}(p,\gamma)^{13}\text{N}$ REACTION

A Yield and Angular Distributions in the Region
of the Giant Resonance

The ninety degree yield for radiative proton capture on ^{12}C was measured for proton energies from 14 MeV to 24.4 MeV (excitation energy in ^{13}N from $E_x = 14.87$ MeV to 24.47 MeV) in steps of 100 keV or smaller. The energy resolution of the beam, including energy losses in the target, was $\cong 15$ keV. The energy resolution of the measured gamma-rays had a full-width half-maximum (FWHM) = 4 %, although the resolution worsened for cases of low yield coupled with a large background due to pile-up. A typical spectrum is shown in figure 4 on page 19.

The gamma-ray from the transition to the ground state (γ_0) was well defined in all the spectra. Gamma-rays from transitions to the second and third excited states at $E_x = 3.51$ MeV and 3.56 MeV could not be resolved, but their sum (γ_{2+3}) was always visible, except where it overlapped with the prolific 15.11 MeV or 12.71 MeV gamma-rays from the inelastic scattering reactions. A significant background was present in the region between γ_0 and γ_{2+3} . This background could be somewhat reduced by decreasing the beam current from ~ 80 nA to ~ 40 nA, implying that it was more pile-up related than neutron related. However, most spectra were taken at ~ 80 nA beam, since the background was still manageable, and decreasing the beam increased running-time prohibitively. Most spectra were taken for an integrated current

TYPICAL SPECTRUM

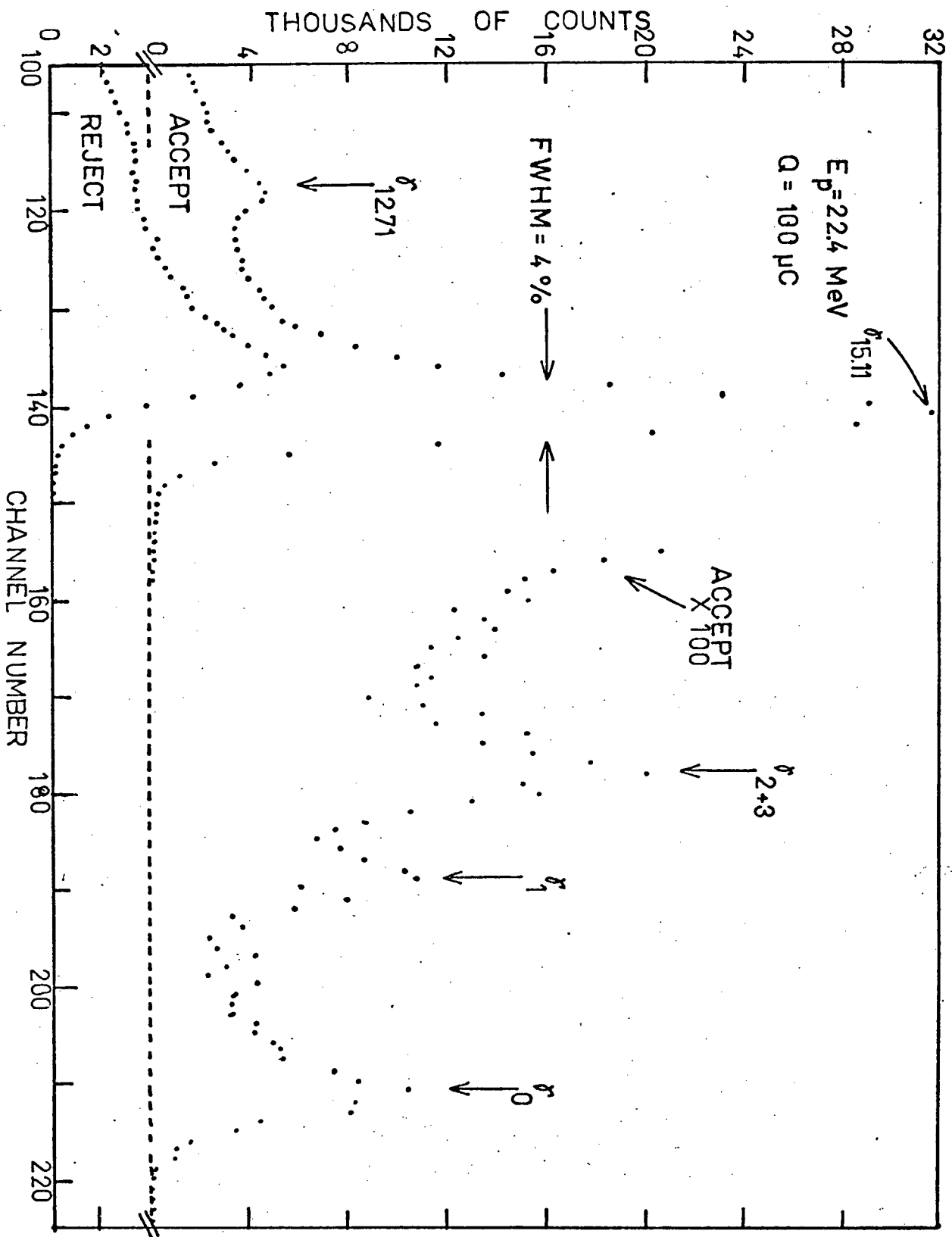


Figure 4

of 100 μC , with a run time of ~ 20 min/spectrum. Gamma-rays from transitions to the first excited state in ^{13}N at $E_x = 2.366$ MeV (γ_1) could be discerned above the background only in the region of the giant resonance ($E_p > 20.5$ MeV).

The data were fitted in several different ways, using the EGG fitting program described in the appendix. For the high energy region ($E_p > 21$ MeV), the capture gamma-rays were well separated from the inelastic gamma-rays. In this region, the three capture gamma-rays ($\gamma_0, \gamma_1, \gamma_{2+3}$) were fit, together with a forced quadratic background. The background was of the form:

$$B(x) = B_0(x - \text{CUTOFF})^2 \quad \text{for } x < \text{CUTOFF}$$

$$B(x) = 0 \quad \text{for } x > \text{CUTOFF}$$

$$\text{CUTOFF} = x_0 - B_1$$

where

x = channel number

x_0 = channel number of γ_0

B_0, B_1 = parameters

Thus, the background is a pure quadratic and goes smoothly to zero at some point above or below γ_0 . This form has the advantage of restricting the amount of background under the photo-peak of the ground state gamma-ray γ_0 , and of not allowing questionable humps that sometimes appear in a cubic background. The parameter B_0 was always allowed to vary, but B_1 was usually fixed at -10.

At lower energies, the γ_{2+3} or γ_1 often overlapped with one of the inelastic gamma-rays. For these energies, γ_0 was fitted either alone or with γ_1 . The fitted region had to be narrowed such that chi-squared was most affected by the lines fit, rather than the background. In all cases, the forced quadratic background was included in the fit. Whenever the γ_1 was fit, it was necessary to fix its excitation energy with respect to the γ_0 .

In overlap regions, the data were fit in several of the above ways. Results were always consistent within the stated errors.

The $^{12}\text{C}(p,\gamma_0)^{13}\text{N}$ yield curve is given in figure 5 on page 222 for proton energy $E_p = 14.3$ MeV to 24.4 MeV. The absolute normalization of the cross-section is uncertain by $\pm 30\%$. The relative errors shown include the statistical error and the uncertainty due to background subtraction as calculated in the error matrix (see appendix and Bevington²⁸).

The main part of the dipole strength appears centered at $E_x = 20.8$ MeV with a width of $\Gamma = 4$ MeV. This roughly coincides with a state seen in proton scattering at $E_x = 20.8$ MeV, with a width $\Gamma = 1.5$ MeV. This state has been assigned a spin and parity $J^\pi = 5/2^+$, based on the analysis of polarization cross-sections by Lowe and Watson,²⁹ and on inelastically scattered proton cross-sections of Scott et al.³⁰ Lowe and Watson state that assignments of $J^\pi = 3/2^+$ and $1/2^+$ are also allowed. Scott compares the measured angular distribution for proton decay to the 15.11 MeV state in ^{12}C

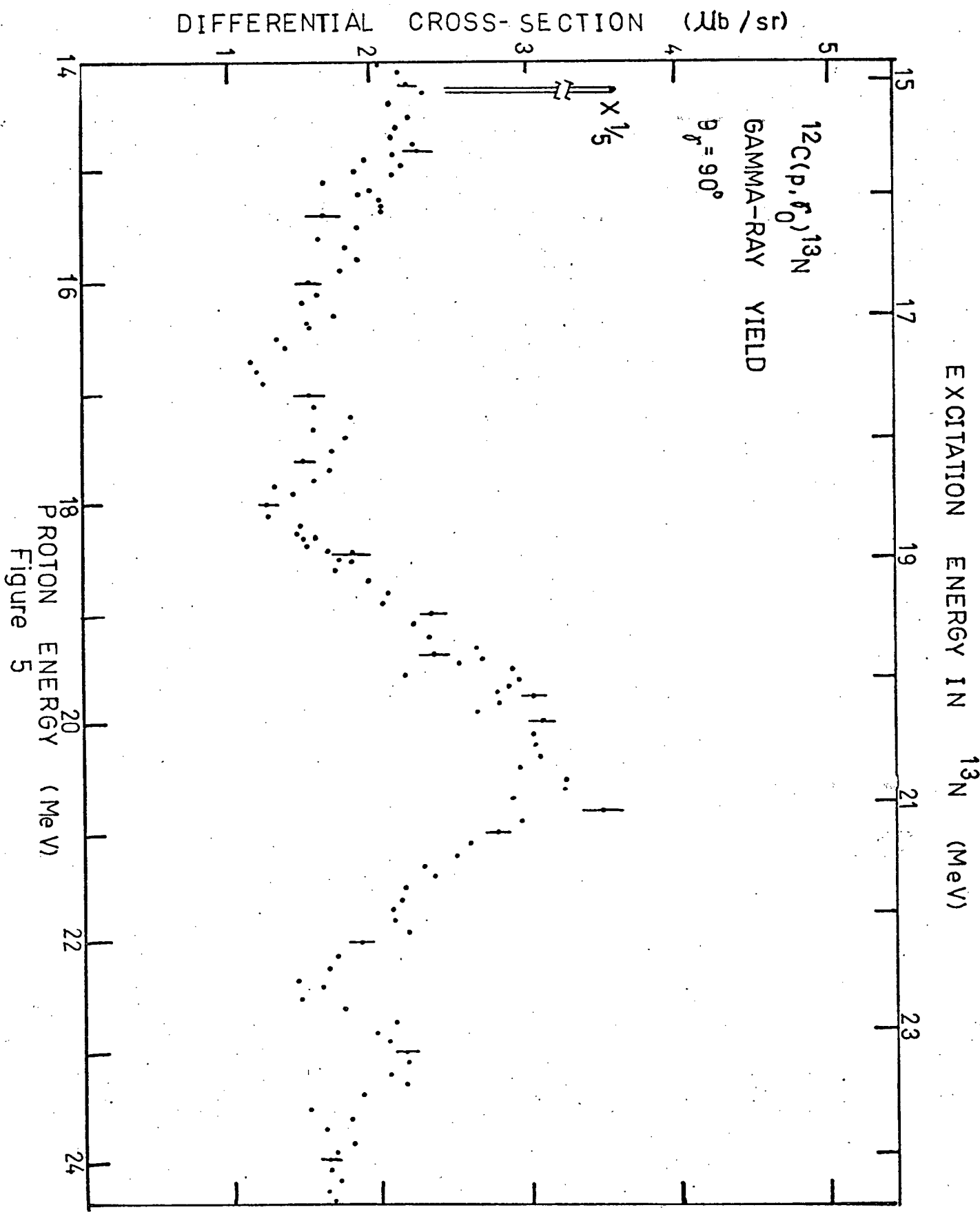


Figure 5

$$\text{expt}(20.5) \longrightarrow P_0 + 0.1 P_1 + 0.8 P_2 - 0.3 P_3 - 0.3 P_4$$

with angular distributions calculated for decays from states of J^π

$$3/2^+ \longrightarrow P_0 + 0.5 P_2$$

$$5/2^+ \longrightarrow P_0 + 0.8 P_2 - 0.1 P_4$$

and conclude $J^\pi = 5/2^+$ is indicated. However, the calculated angular distributions of Scott are based on the assumption that different channel spins contribute equally to the cross-sections. This assumption is reasonable in the sense that, in the absence of a detailed model for the reaction mechanism, we can do no better. It has, however, a very significant effect on the calculated angular distributions. Our calculations of the angular distributions for each channel spin are given in table I on page 24. We see that no combination of channel spins for $J^\pi = 5/2^+$ can adequately account for the measured values of both a_2 and a_4 (different channel spins do not interfere). Other interference effects must be important. A resonance of $J^\pi = 3/2^+$ can easily account for the large a_2 value. The non-zero value of a_4 indicates interference with a resonance of $J \geq 5/2$ with positive parity, but this is not unlikely. If this state contributes to the γ_0 yield, as seems likely, an assignment of $J^\pi = 3/2^+$ is strongly indicated. This assignment is not inconsistent with existing proton scattering data. We cannot rule out the possibility that two separate resonances are superimposed.

Table I

Angular distributions for protons scattered inelastically to the $J^\pi = 1^+$ state at 15.11 MeV in ^{12}C , calculated in the channel-spin coupling scheme. J^π refers to the compound nuclear state, L to the scattered proton. S is the channel spin.

J^π	L	S	Angular Distribution
$3/2^+$	2	1/2	$4 (P_0 + P_2)$
		3/2	$4 P_0$
$5/2^+$	2	1/2	$6 (P_0 + 1.14 P_2 + 0.86 P_4)$
		3/2	$6 (P_0 + 0.41 P_2 - 0.97 P_4)$

The region $E_p = 16.5$ MeV to 18.5 MeV in the γ_0 yield probably contains further structure. Whether this should be interpreted as two dips or a separate peak is not clear. The high density of states seen in inelastic proton scattering in this region¹⁰ would support almost any hypothesis. Angular distributions in this region might provide some insight, however these have not yet been obtained.

Whether the slowly increasing yield down to $E_p = 14$ MeV joins smoothly to the pygmy resonance at $E_p = 10$ MeV to 13 MeV or is a separate bump is another unresolved question. Further measurements in this region gave some indication that the yield reaches a minimum near 14 MeV, but because of time constraints, the statistics were rather poor and did not warrant a definitive statement. A broad background seems to underlie the entire yield curve.

The sharp peak at $E_p = 14.231$ MeV is a $T = 3/2$ state. This very narrow resonance was found in the $^{11}\text{B}(^3\text{He},n)^{13}\text{N}$ reaction, and also in the mirror reaction $^{11}\text{B}(^3\text{He},p)^{13}\text{C}$. The anomaly is also seen in proton scattering data.²⁰ A spin-parity assignment of $J^\pi = 3/2^+$ was confirmed by the $^{12}\text{C}(p,\gamma_0)$ data of Dietrich et al.¹⁷ Szucs et al.³¹ have measured the full width and found $\Gamma = 1.3 \pm 0.3$ keV. Adelberger et al., 1973,³² have found $\Gamma = 0.82 \pm 0.2$ keV by a coincidence ($^3\text{He},n\gamma$) measurement, in good agreement with the previous result. The width, spin and parity, M1 decay width, and other information about this state all indicate that it is the lowest $T = 3/2$ level in ^{13}N , the

analogue of the ground state of ^{13}B and ^{13}O . This resonance was used to measure the target thickness.

^{13}N has two narrow $T = 3/2$ resonances at $E_x = 17.86$ MeV and 18.46 MeV. These states primarily proton decay to the $T = 1/2$ 15.11 MeV level in ^{12}C , and are seen in the yield of that gamma-ray (see section IV A). These regions were examined in 25 keV steps, but no corresponding structure was seen in the γ_0 yield. This might indicate a many particle-hole configuration.

The structure above the main strength of the GDR is quite interesting. It might be interpreted as a dip at $E_p = 22.4$ MeV or as a peak at $E_p = 23$ MeV. Angular distributions were performed at $E_p = 22.4$ MeV and 23.2 MeV. The results are shown in figure 6 on page 27, together with the fitted Legendre polynomial coefficients according to the equation:

$$Y(\theta) = A_0 \left(1 + \sum_{i=1}^n a_i P_i(\cos\theta) \right)$$

by the program LEGFIT (see appendix). An asterisk (*) above the coefficients indicates the fit was forced to be non-negative at either forward or backward angles.

At these energies, the yield was taken at only five angles between 60° and 124° . Still, the results are quite striking. All three capture gamma-rays are strongly asymmetric about ninety degrees. The γ_0 and γ_{2+3} are less asymmetric (smaller a_1) at 23.2 MeV than at 22.4 MeV (the γ_1 is less well defined). The 15.11 MeV gamma-ray from the inelastic reaction is moderately anisotropic at 22.4 MeV, but becomes very nearly isotropic at 23.2 MeV.

ANGULAR DISTRIBUTIONS
AT 224 MeV AND 23.2 MeV

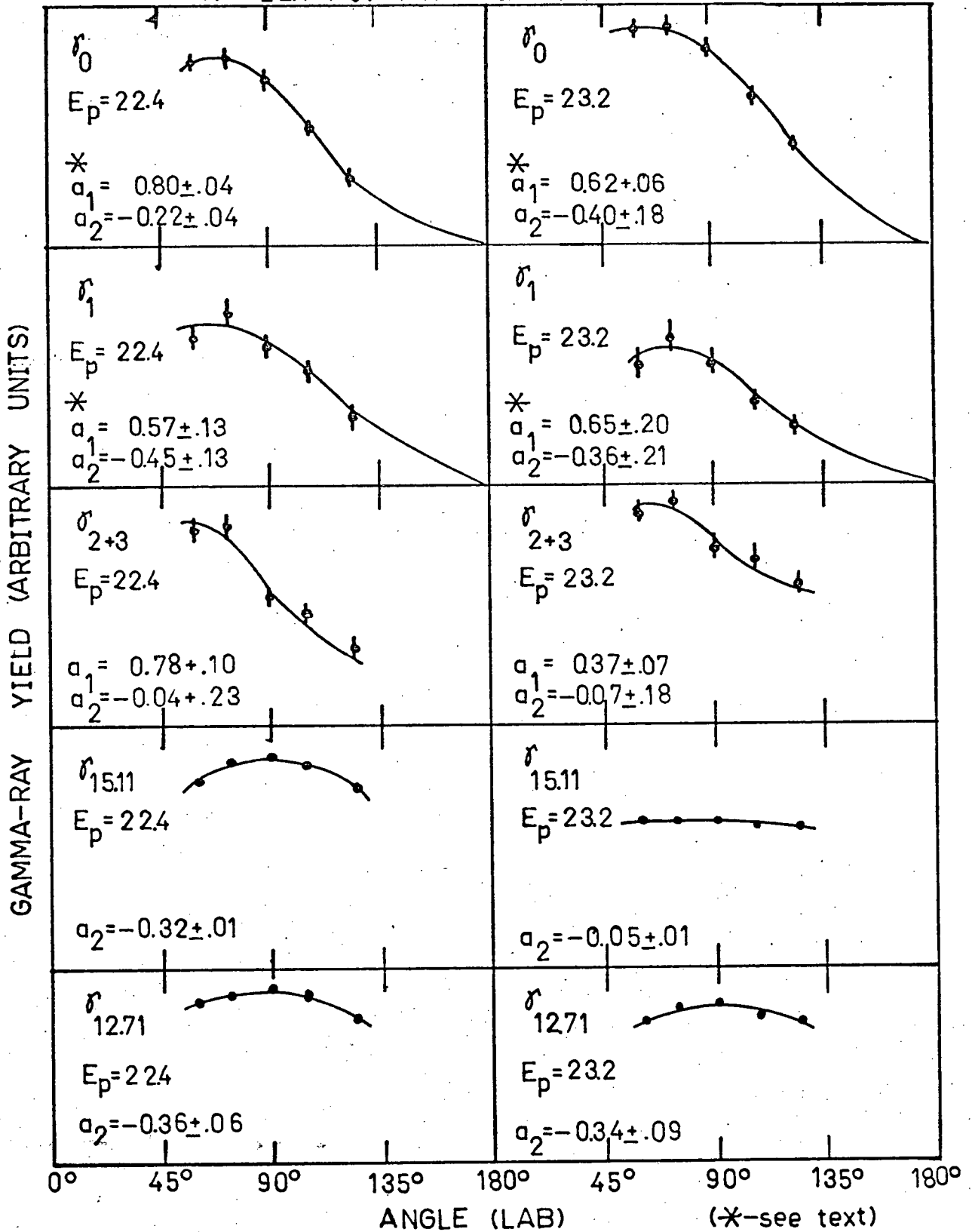


Figure 6

The asymmetry in the capture gamma-rays indicates that levels of opposite parity are interfering. Assuming the dipole resonance is primarily $J^\pi=3/2^+$, one could hypothesize that the other level is the $5/2^-$ state at $E_p = 22.4$ MeV, seen as a broad shoulder in the 15.11 MeV and 12.71 MeV yields (see section IV A) and identified through the analysis of elastic scattering and polarization cross-sections by Lowe and Watson, 1966.²⁹ This would give E1-E2 interference in transitions to the ground state, and would account for the observed angular distributions (see table II on page 37). However, since E1-E2 interference gives rise only to odd legendre polynomials, this interference would not account for a dip in the ninety degree γ_0 yield. Possible explanations for this structure are considered in section V.

The γ_1 ninety degree yield is given as figure 7 on page 29 for proton energies from $E_p = 19.8$ MeV to 24.4 MeV. To simplify the fitting procedure, the excitation energy of the γ_1 was always held fixed with respect to the γ_0 . At lower energies, this gamma-ray is lost in a pile-up associated background. The giant resonance in the γ_1 yield is centered near a gamma-ray energy $E_g = 19.5$ MeV and has a width $\Gamma = 2.5$ MeV. The yield seems to increase quite sharply at $E_p = 20.5$ MeV, but the error bars are large, and the actual effect may not be so dramatic. No fine structure was detected.

The γ_{2+3} yield is given as figure 8 on page 30 from $E_p = 19.7$ MeV to 24.4 MeV, along with earlier results of Fisher et al., 1963,¹⁶ at higher proton energies. The results of Fisher have been re-normalized to agree with the present results. At lower

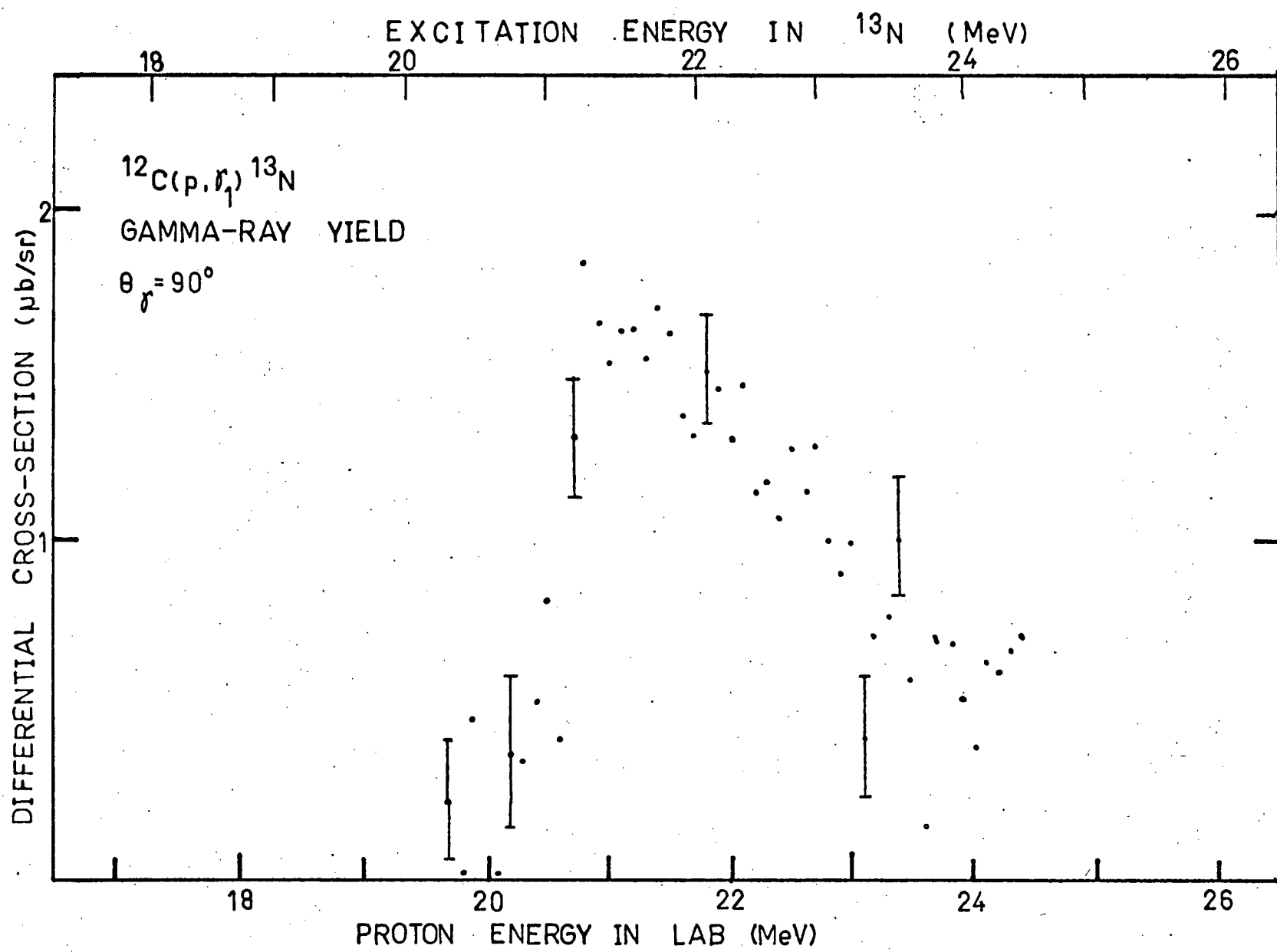


Figure 7

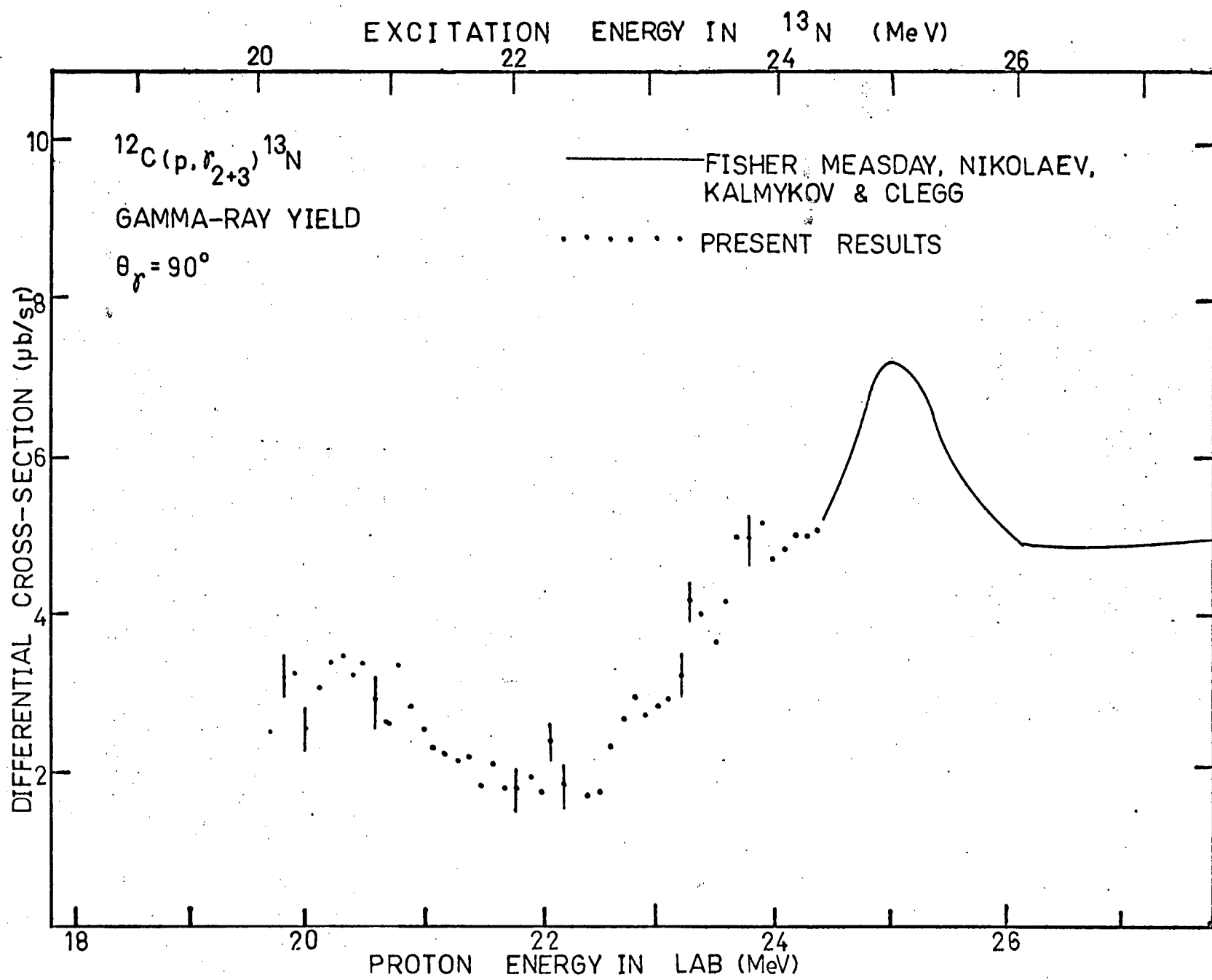


Figure 8

proton energies, the γ_{2+3} overlays the inelastic gamma-rays, and cannot be extracted reliably. No fine structure is apparent. The yield goes through a minimum near $E_p = 22$ MeV. The increase at lower energies might indicate the presence of the pygmy resonance. At higher energies, the yield approaches the giant resonance, as seen by Fisher.

B Angular Distributions in the Region of the
Pygmy Resonance

Radiative proton capture on carbon-12 in the region $E_p = 9$ MeV to 15 MeV was previously studied by Measday, Hasinoff, and Johnson, 1973.¹⁹ Measday found two dramatic dips in the γ_0 yield at $E_p = 10.62$ MeV and 13.12 MeV. Their yield is reprinted as figure 9 on page 33. The two dips were fit quite well as narrow resonances of width $\Gamma = 200$ keV interfering with the broad background of the pygmy resonance. However, the ninety degree yield does not tell us with certainty whether there is a dip in the total cross-section, or only a rapid variation in the angular distribution. Also, the decrease in yield could be due to a resonance in some competing reaction channel depopulating the state. To further understand this phenomena, angular distributions were obtained in the region of the pygmy resonance.

Angular distributions were measured at six energies, indicated by arrows in figure 9. At each energy, the yield was measured at six angles between 45° and 135°. The angular distributions for γ_0 are given in figure 10 on page 34. The fitted Legendre polynomial coefficients defined by the equation:

$$Y(\theta) = A_0 \left(1 + \sum_{i=1}^n a_i P_i(\cos\theta) \right)$$

for $n = 2$ are given at each energy. Where values have been preceded by an asterisk (*), the fit has been forced to be non-negative. The angular distributions are all peaked near ninety

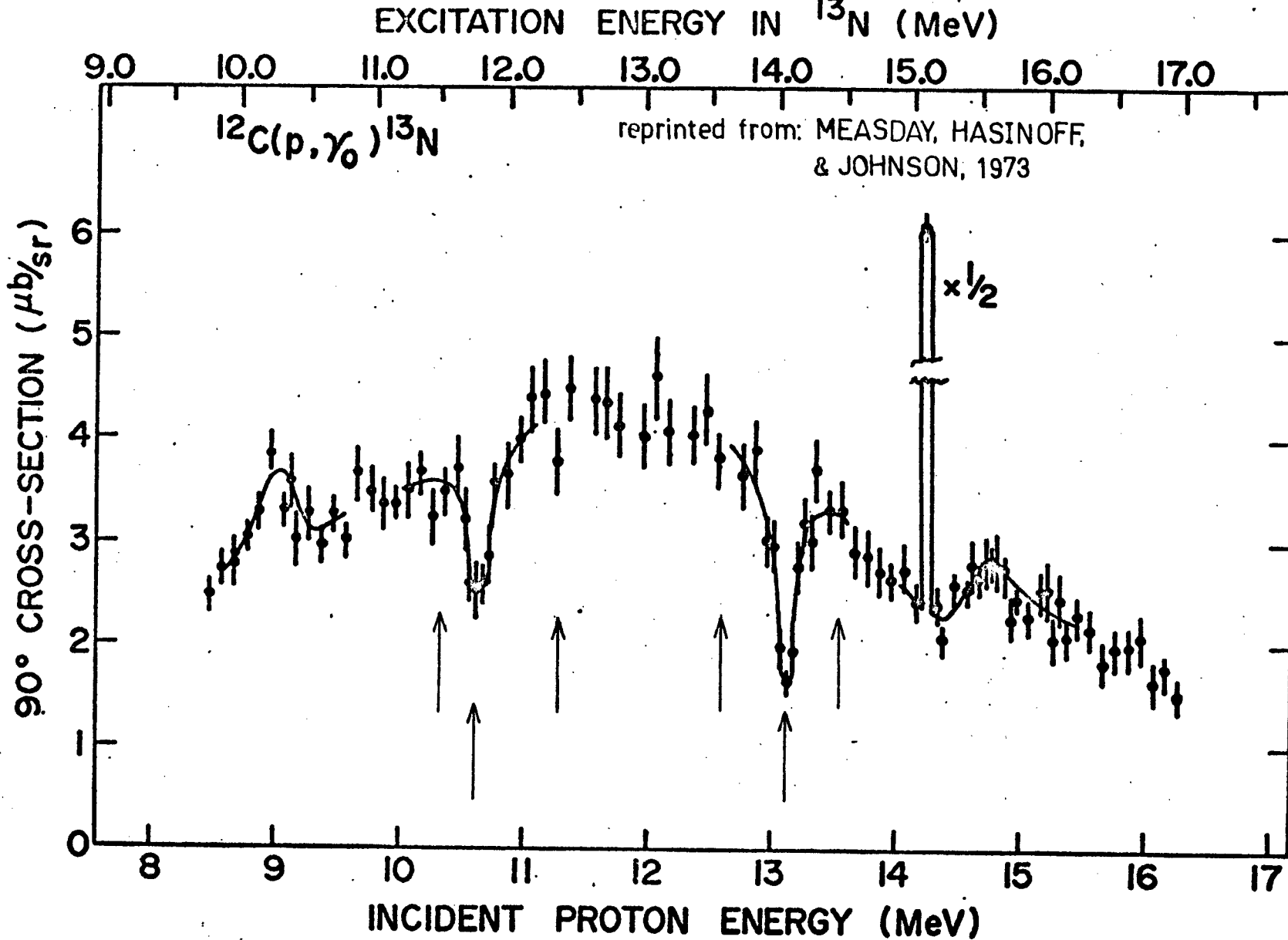


Figure 9

γ_0 ANGULAR DISTRIBUTIONS IN THE PYGMY RESONANCE

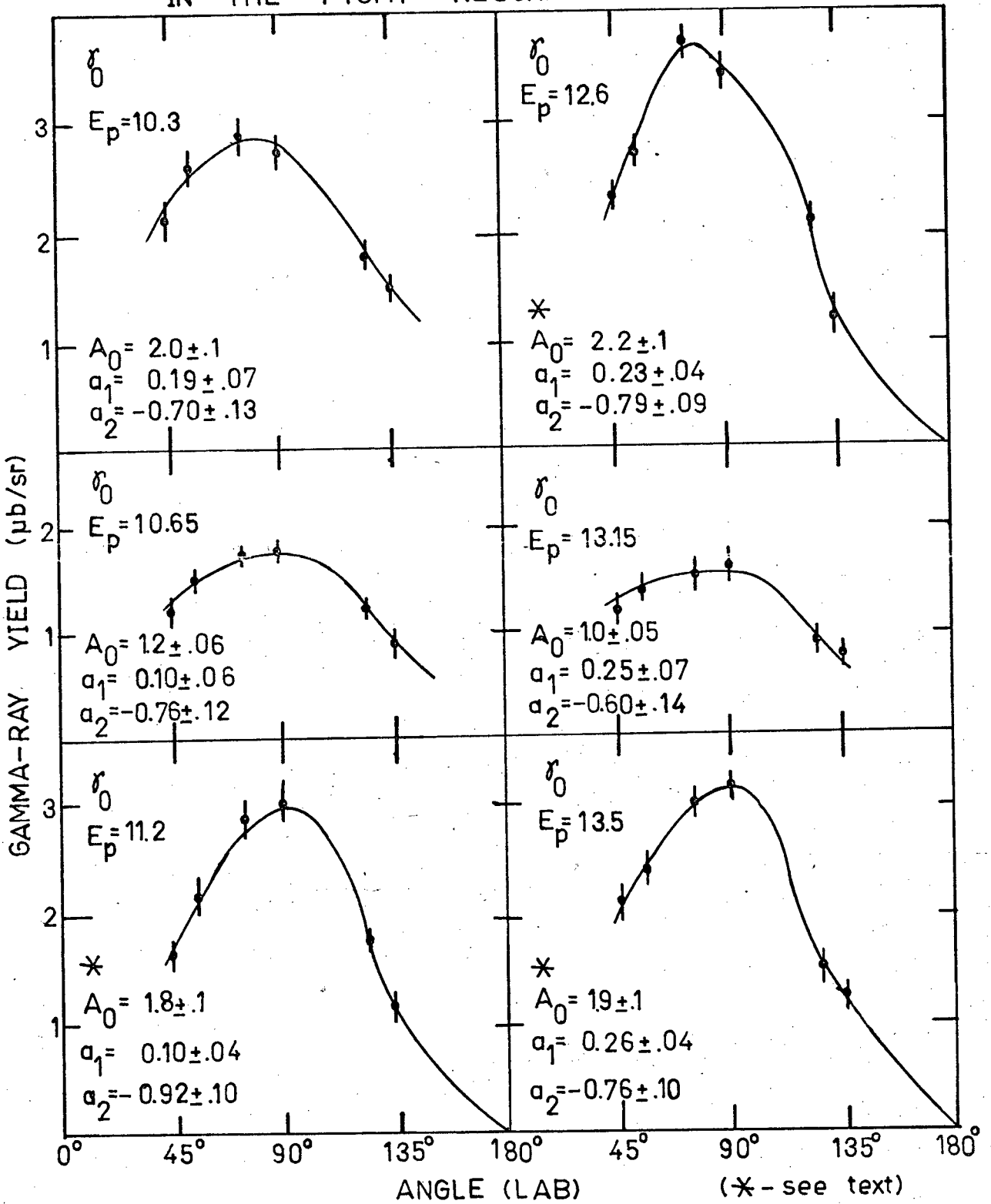


Figure 10

degrees. All are slightly asymmetric.

The fitted Legendre polynomial coefficients are plotted in figure 11 for the fits performed with $n = 2$ and $n = 4$. The values for the γ_0 angular distributions measured at $E_p = 22.4$ MeV and 23.2 MeV have also been included. The errors shown are those calculated in the error matrix (see appendix). Including the third and fourth-order Legendre polynomials does not significantly improve the fit according to F-test²⁸ (with the possible exception of the $E_p = 13.5$ MeV angular distribution). The truncated angular region allowed by the experimental set-up does not well define the higher order coefficients, which results in very large errors for the $n = 4$ fit. Knowledge of the yield at far forward or backward angles is necessary to better determine the a_3 and a_4 coefficients.

The Legendre fits with $n = 2$ were adequate, overall. As figure 11 illustrates, the a_1 and a_2 coefficients are nearly constant throughout this region. The only dramatic variation occurs in the A_0 coefficient, i.e. the dips do occur in the integrated cross-section.

Calculated angular distributions for γ_0 from radiative proton capture in the channel spin coupling scheme are given in table II on page 37 for E1, M1, and E2 radiation, and for E1-E1, M1-M1, E2-E2, E1-E2, and E1-M1 interference terms. Because the target nucleus has $J^\pi = 0^+$, the j-j and L-S coupling schemes give distributions which differ by only an overall normalization. Assuming this is dipole radiation, the strongly

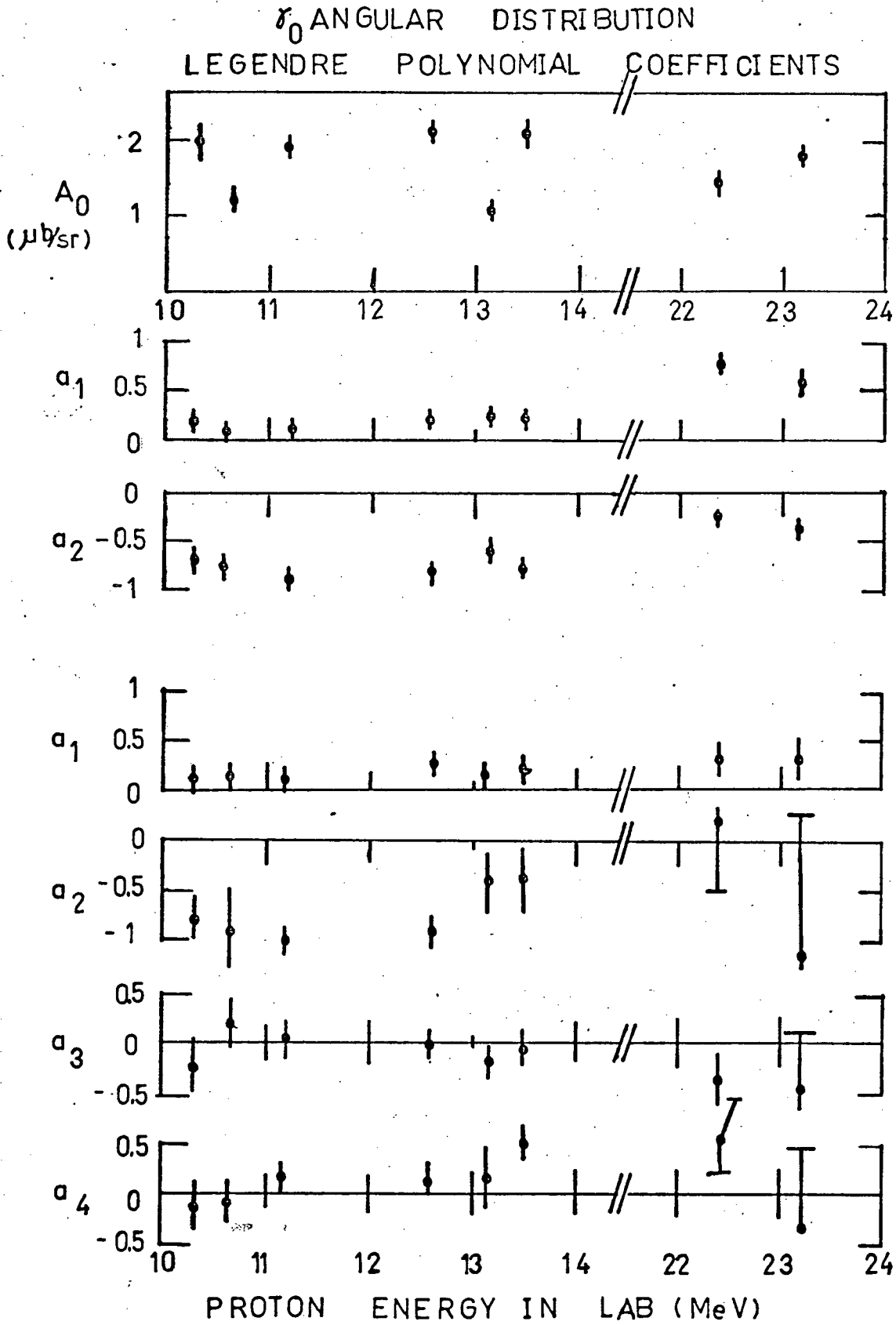


Figure 11

Table II

Calculated gamma-ray angular distributions for the $^{12}\text{C}(p,\gamma_0)$ reactions as a function of l and j of the incoming proton in the channel spin coupling scheme.

<u>l</u>	<u>j</u>	<u>type</u>	<u>Angular Distribution</u>
0	1/2	E1	2 P ₀
2	3/2	E1	4 (P ₀ - 0.5 P ₂)
1	1/2	M1	2 P ₀
1	3/2	M1	4 (P ₀ - 0.5 P ₂)
1	3/2	E2	4 (P ₀ + 0.5 P ₂)
3	5/2	E2	6 (P ₀ + 0.57 P ₂ - 0.57 P ₄)

Interference Terms

<u>l</u>	<u>j</u>	<u>type</u>	<u>l</u>	<u>j</u>	<u>type</u>	<u>Angular Distribution</u>
0	1/2	E1	2	3/2	E1	2 P ₂
1	1/2	M1	1	3/2	M1	-2 P ₂
1	3/2	E2	3	5/2	E2	-0.86 (P ₂ - 8 P ₄)
0	1/2	E1	1	1/2	M1	-2 P ₁
0	1/2	E1	1	3/2	M1	2 P ₁
2	3/2	E1	1	1/2	M1	-2 P ₁
2	3/2	E1	1	3/2	M1	2 P ₁
0	1/2	E1	1	3/2	E2	1.15 P ₁
0	1/2	E1	3	5/2	E2	1.15 P ₃
2	3/2	E1	1	3/2	E2	0.69 (P ₁ - 6 P ₃)
2	3/2	E1	3	5/2	E2	6.2 (P ₁ - 0.44 P ₃)

negative a_2 value indicates $J^\pi = 3/2^+$ for the pygmy resonance. This is an expected result, as non-spin-flip E1 transitions are favored over spin-flip E1 transitions.³³ That the measured value $a_2 = -0.75$ is more negative than the predicted $a_2 = -0.5$ probably indicates some degree of background, as does the small non-zero a_1 value.

As the calculated angular distributions illustrate, the integrated cross-section (which depends only on the A_0 coefficient) can be influenced by interfering resonances only if they have the same angular momentum and parity. Interfering levels with the same parity, but different angular momentum affect the higher order even coefficients. Interfering levels of opposite parity introduce odd Legendre polynomials. Thus, if the structure is caused by two narrow resonances interfering with the broad pygmy resonance, our results indicate their angular momentum and parity must be $J^\pi = 3/2^+$, to agree with the pygmy resonance.

As noted by Measday et al., 1973,¹⁹ the dip at $E_p = 10.62$ MeV coincides with a level seen in the elastic and inelastic scattering of polarized protons on carbon-12 by Meyer and Plattner, 1973.²¹ This resonance, at $E_x = 11.75$ MeV, has a width $\Gamma = 250$ keV, and was ascribed $J^\pi = 3/2^+$ by phase shift analysis. Although some of the results of Meyer and Plattner have been questioned by Measday, this exceptional agreement in position, width, angular momentum and parity of the resonance lends some weight to the interpretation of the dip as an interference effect.

We note also that fine structure of approximately this width was seen in this region in the yield of the 4.43 MeV gamma-ray from the inelastic reaction in the earlier data of Adams et al, 1961.³⁴

The minimum at $E_x = 14.04$ MeV, also as noted by Measday, could perhaps be identified with a level at $E_x = 13.96 \pm .05$ MeV with $\Gamma = 150$ keV, $J^\pi = 3/2^+$, seen in the elastic scattering data of Levine and Parker, 1969.²⁰

The alternative interpretation of the dips being caused by a resonance in some competing reaction cannot be completely ruled out. A competing reaction would not be expected to affect the angular distribution, which is still consistent with our results. The only channel open at this energy, besides the entrance channel and radiative decay, is $^{12}\text{C}(p, \alpha)^9\text{B}$. This reaction has a threshold of $E_p = 9.5$ MeV. Unfortunately, a yield curve in this region does not exist. Levine and Parker²⁰ have examined this reaction near the $T = 3/2$ resonance at $E_p = 14.231$ MeV, but not at lower energies. They did note several correlations in the (p, p') and (p, α') reactions at higher energies. However, the α decay widths usually never vary as dramatically as would be necessary to account for the minima in the region of the pygmy resonance.

The pygmy resonance is often thought to arise from transitions involving the valence nucleon. For a valence nucleon dipole transition to the ground state of ^{13}N to occur, the incoming proton would have to fall into a $d_{3/2}$ or $s_{1/2}$ shell orbital.

The measured angular distributions in the region of the pygmy resonance are consistent with an incoming $d_{3/2}$ proton (see table II), although transitions from a many particle-hole state cannot be ruled out. Some relevant theoretical calculations are discussed in section V.

IV YIELDS OF THE 12.71 MeV AND 15.11 MeV GAMMA-RAYS

FROM THE INELASTIC REACTION $^{12}\text{C}(p,p'\gamma)^{12}\text{C}^*$

The two $J^\pi = 1^+$ energy levels in ^{12}C at 12.71 MeV ($T = 0$) and 15.11 MeV ($T = 1$) both have shell model configurations $(p_{3/2})^{-1}(p_{1/2})^1$. When viewed as lp-lh states, with the ^{12}C core as the vacuum, the 12.71 MeV level is symmetric in the spin component of its wavefunction; and anti-symmetric in its iso-spin component, and the 15.11 MeV level is anti-symmetric in spin and symmetric in iso-spin. Together, these levels exhaust the $J^\pi = 1^+$ strength in the lp shell and are well isolated from the next 1^+ configuration-- $(sd)^2(p)^{-2}$.

Table III on page 42 lists the known decay widths of these levels. The 12.71 MeV level alpha decays mainly to the 2.90 MeV first excited state ($J^\pi = 2^+$, $T = 0$) in ^8Be , even though the decay is inhibited by a factor of $\sim 10^4$. (The 12.71 MeV level is viewed as a lp-lh state, whereas alpha decay couples to 4p-4h configurations.) Decay to the ground state in ^8Be is prohibited by conservation of parity and angular momentum, thus gamma decay accounts for the remaining 3 % of the total width. 85 % of this gamma width is M1 radiation to the ground state of ^{12}C . The total cross-section for excitation of the level was calculated using a branching ratio

$$\Gamma_{\gamma_0} / \Gamma = (2.5 \pm .3) \% \quad 37$$

and assuming an isotropic angular distribution.

Table III

Decay widths of the 12.71 MeV and 15.11 MeV gamma-rays

Energy ^a	$J^\pi(T)$ ^a	total width Γ (eV)	alpha width Γ_α/Γ (%)	gamma-ray decays (%)			
				to ground $\Gamma_{\gamma'}/\Gamma$	to 4.4 MeV $\Gamma_{\gamma'}/\Gamma_\gamma$	to 7.7 MeV $\Gamma_{\gamma'}/\Gamma_\gamma$	to 12.7 MeV $\Gamma_{\gamma'}/\Gamma_\gamma$
12.713 \pm .006	1 ⁺ (0)	14.6 \pm 2.8 ^b	97.1 \pm .3 ^c	2.4 \pm .3 ^b	17. \pm .3 ^c	<10. ^c	—
15.109 \pm .004	1 ⁺ (1)	39.4 \pm 1.5 ^a	3.6 \pm 2.8 ^d	95. \pm .3 ^e	1.5 \pm .3 ^c	1.5 \pm .2 ^c	0.7 \pm .3 ^c

a) Ajzenberg-Selove and Lauritsen, 1968³⁵b) Cecil et al., 1974³⁶c) Riesman et al., 1970³⁷d) Adelburger and Busoletti, 1973³⁸e) Chertok et al., 1973³⁹

The 15.11 MeV level is the first $T = 1$ state in ^{12}C , the analogue of the ground states of ^{12}B and ^{12}N . Although the state is 7.7 MeV above the alpha break-up threshold, alpha decay is isospin forbidden, and the state decays via gamma emission almost entirely. The ground state branching ratio is very large ($\Gamma_\gamma/\Gamma \geq 92\%$), although there is some disagreement on its exact value (see Riesman et al.,³⁷ and Alburger and Wilkinson, 1972⁴⁰). The 15.11 MeV level could alpha decay via some isospin impurity, i.e. mixing of the 12.71 MeV and 15.11 MeV levels. This mixing is thought to occur with an amplitude of $\sim 11\%$.^{38,41} Still, the alpha decay branching ratio of the 15.11 MeV level is probably less than 2%. For our calculations, we assume $\Gamma_{\gamma_0}/\Gamma = 1$ and derive the angular distributions from the a_2 values given by figure 13 on page 58.

A Yield of the 15.11 MeV Gamma-Ray

The 15.11 MeV gamma-ray yield curve is given in figure 12 for proton energies from threshold ($E_p = 16.39$ MeV) to 24.4 MeV. The uncertainty in absolute normalization is ± 30 %. Throughout this region, the 15.11 MeV gamma-ray is the most prominent feature of the spectrum. No background subtraction was necessary when the 15.11 MeV and 12.71 MeV gamma-rays were fit together. The yield curve duplicates quite well the recent results of Measday et al., 1973,¹⁹ and Ebisawa et al., 1973.⁴²

The narrow $T = 3/2$ resonances in ^{13}N at $E_p = 17.86$ MeV and 18.46 MeV are clearly seen. These states can proton decay to the 15.11 MeV level, but are prohibited from decaying to the 12.71 MeV level by isospin conservation. (We would estimate

$\Gamma_{p12.71} / \Gamma_{p15.11} < 50$ % for both resonances.) The resonance at $E_p = 17.3$ MeV, previously seen by Snover et al.,^{43,35} has a slightly deformed shape, which is presumably a threshold effect. The most prominent features of the yield are the two well defined peaks at approximately $E_p = 19.4$ MeV and 20.5 MeV, together with the broad shoulder at about 22.4 MeV. The yield seems to level off at about 23.6 MeV. The yield at these energies would include contributions from peaks at higher energies, in particular the resonance seen at $E_p = 25.5$ MeV in the DWBA analysis of inelastic proton scattering data by Scott et al., 1967,³⁰ and in agreement with the earlier gamma-ray data of Measday et al.⁴⁴

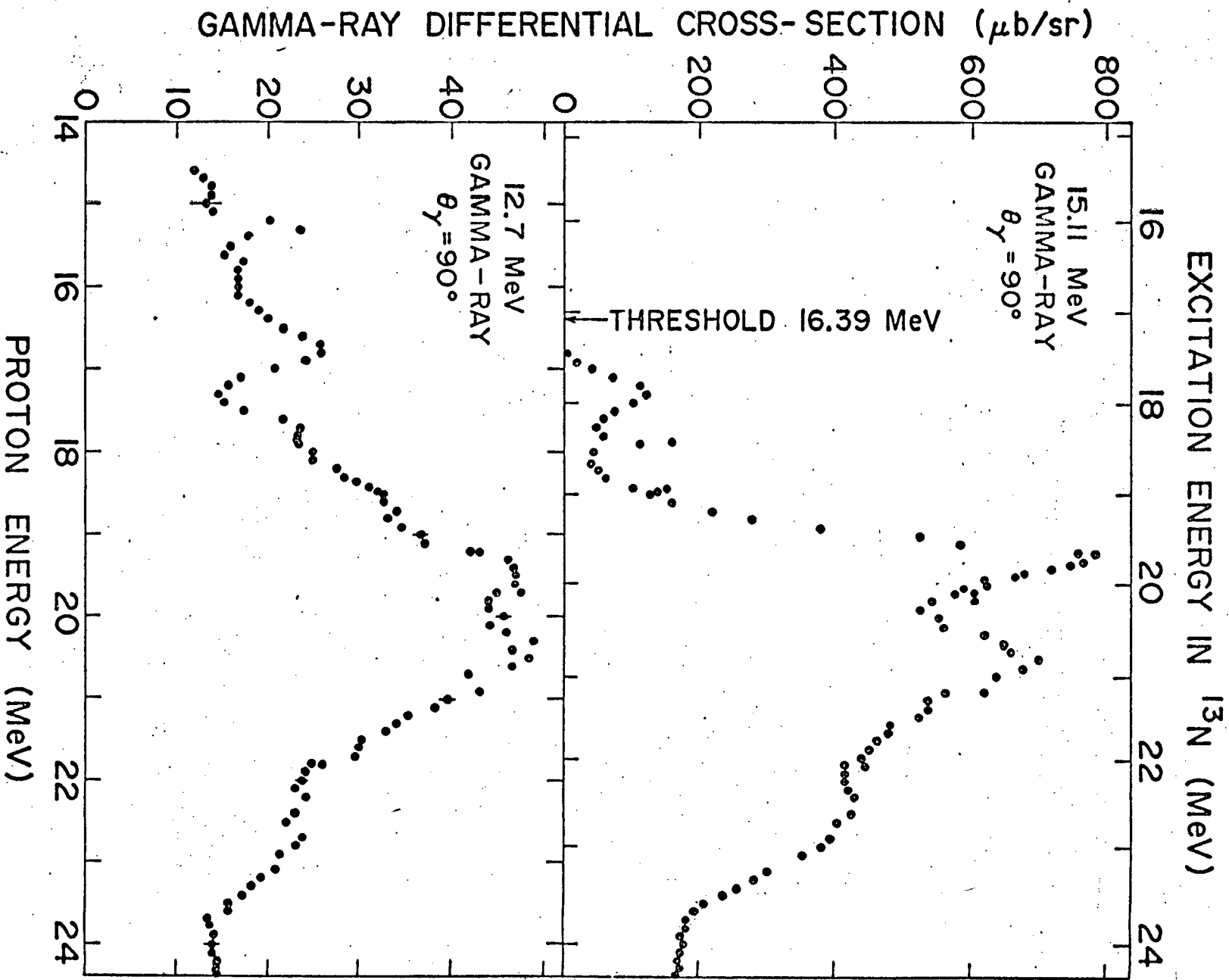


Figure 12

The yield curve was fit in segments with two interfering Breit-Wigner resonance shapes, using the program of Hasinoff (described in the appendix). Results of this fitting are given in table IV on page 47. The pairs of values quoted are the "strong" and "weak" solution discussed in the appendix. The brackets indicate resonances fit as interfering pairs. Within any bracket, all the first solutions or all the second solutions are self-consistent (unless otherwise noted). The third value, if given, is an estimate of the proton widths assuming no interference and some reasonable background subtraction.

A non-interfering background is possibly present under some of the fitted peaks. For the 15.11 MeV yield, these are the 19.4 MeV, 20.5 MeV and 22.4 MeV peaks. Rather than treat the non-interfering background as a free parameter, three special cases were fit: 1) no non-interfering background, 2) one-half the maximum possible non-interfering background, and 3) the maximum possible non-interfering background. For the peaks in the 15.11 MeV yield, the maximum background was estimated to be $\sim 170 \mu\text{b}/\text{sr}$. The proton widths quoted are those that seemed most reasonable, with total widths most nearly the accepted values. However, the quoted errors include the uncertainty in the background subtraction.

The peaks at $E_p = 17.3 \text{ MeV}$ and 17.9 MeV were fit together, but appear essentially non-interfering. The other $T = 3/2$ resonance at $E_p = 18.46 \text{ MeV}$, although clearly discernable, could not be fit adequately. (One might guess $\Gamma_p < 1.5 \text{ keV}$.)

Table IV

Resonances in ^{13}N found in the yield of the 12.71 MeV and 15.11 MeV gamma-rays.*

E_p (MeV)	E_x (MeV)	J^π (T) ^a	total width Γ (keV)	proton widths (keV)		
				ground state	12.71 MeV level	15.11 MeV level
15.27	16.02	$7/2^+$	$102 \pm 10 \%$	7.5^b	$4.2 \pm 10 \%$ $98. \pm 10 \%$ $14. \pm 20 \%$	— — —
17.3	17.9	?	$594 \pm 5 \%$ $401 \pm 5 \%$	40^c	$50. \pm 20 \%^d$ $1100 \pm 30 \%^d$? $46 \pm 20 \%^d$
17.9	18.46	$3/2^+$ (3/2)	$101 \pm 30 \%$	25^b	—	$1.8 \pm 10 \%$? $2.5 \pm 20 \%$
18.8	19.3	?	$500 \pm 100 \%$	50^c	$320 \pm 100 \%^d$ $3640 \pm 20 \%^d$ $260 \pm 50 \%^d$?
19.4	19.83	$5/2^-$ (1/2)	$1000 \pm 50 \%$ $1500 \pm 50 \%$	175^b	$21.7 \pm 50 \%$ $230 \pm 50 \%$ $230 \pm 50 \%$?
19.46	19.88	$3/2^+$ (1/2)	$506 \pm 4 \%$ $730 \pm 2 \%$	208^b	?	$11.4 \pm 20 \%$ $32.6 \pm 20 \%$ $30 \pm 20 \%$
20.5	20.9	$5/2^+$ ^f (?)	$1504 \pm 4 \%$	200^g	$520 \pm 100 \%$ $300 \pm 100 \%$ $500 \pm 50 \%$	$169 \pm 20 \%$ $65 \pm 20 \%$ $360 \pm 20 \%$
22.4	22.6	$5/2^-$ ^f (?)	$1300 \pm 25 \%$	50^g	$240 \pm 100 \%$? $600 \pm 50 \%$	$100 \pm 50 \%$ $1000 \pm 50 \%^h$ $160 \pm 30 \%$

* references are on the following page.

References for table IV:

- a) Given by Ajzenber-Selove,¹⁰ unless otherwise noted
- b) Levine and Parker²⁰
- c) We estimate $\Gamma_{p_0} / \Gamma = 10 \%$
- d) Divide by statistical spin factor $g(s) = \frac{2s+1}{2} > 1$
- e) Only consistent with $\Gamma_p = 2300$ keV for the 19.4 MeV resonance
- f) Assumed from the optical model of Scott et al.³⁰
- g) Estimated, see Lowe and Watson²⁹
- h) Only consistent with $\Gamma_p = 400$ keV for the 20.5 MeV resonance

The fit of the peak at $E_p = 19.4$ MeV yielded a width $\Gamma = 500$ keV to 750 keV, which would indicate that the major contributor is the resonance at $E_p = 19.46$ MeV ($E_x = 19.88$ MeV, $\Gamma = 520$ keV). For the set of interfering solutions given for the peaks at $E_p = 19.4$ MeV, 20.5 MeV, and 22.4 MeV, the upper values would seem the most believable, being the closest to the non-resonant estimates. Note, however, that the second set is not entirely ruled out. A value of $\Gamma_p = 1000$ keV for the 22.4 MeV peak seems unlikely, but the requirement that the 20.5 MeV state have a width of 400 keV could conceivably reflect a contribution from the 19.4 MeV state, if this was the broader ($\Gamma = 1000$ keV) $J^\pi = 5/2^-$ level, rather than the $J^\pi = 3/2^+$ state, as suggested. Also, for the 22.4 MeV peak, subtraction of the non-interfering background causes considerable uncertainty in the proton widths, which is included in the stated errors. Note, however, that if the 22.4 MeV resonance has $J^\pi = 5/2^-$, as suggested in the analysis of the elastic scattering data by Lowe and Watson,²⁹ one would not expect to see any interference effects with the positive parity states at $E_p = 20.5$ MeV and 19.46 MeV in the ninety degree yield. The spin and parity assignment of the 20.5 MeV level is based on the optical model phase shift analysis of elastic scattering and polarization cross-sections done by Lowe and Watson, and is supported by the inelastic scattering data and analysis of Scott et al.³⁰ The spin assignment was questioned in section III A, page 23,

of this report. The spin and parity of the $E_p = 19.46$ state was determined by Levine and Parker,²⁰ by optical model phase-shift analysis of lower energy scattering data.

We note some disagreement in the reported values of the energies and widths of the two $T = 3/2$ states. Snover et al.⁴³ report $E_x = 18.42$ MeV and 18.97 MeV with $\Gamma = 66 \pm 8$ keV and 23 ± 5 keV respectively, as given by Ajzenberg-Selove.¹⁰ Levine and Parker²⁰ report $E_x = 18.35$ and 18.96 MeV with $\Gamma = 100$ keV and 15 keV. We give a value of $\Gamma = 100$ keV for the former resonance, but this is with no background subtraction. Some background subtraction seems likely, and this would lower our value to a better agreement with Snover. Our energy scale was calibrated using the energy of the lowest $T = 3/2$ level, which is quite well known. Our results give the energy for this level as $18.456 \pm .015$ MeV, also in agreement with Snover. Because of our target thickness and the quality of our data in the region of the 18.96 MeV state, we cannot further comment on that discrepancy.

B Yield of the 12.71 MeV Gamma-Ray

The 12.71 MeV yield curve is also given in figure 12 on page 45 for proton energies from 14.6 MeV to 24.4 MeV ($E_x = 15.4$ MeV to 24.5 MeV). There is an uncertainty of approximately $\pm 30\%$ in the absolute normalization. Above a proton energy of 16.8 MeV, the 12.71 MeV gamma-ray sits on the tail of the 15.11 MeV gamma-ray. These spectra were fit with only the 12.71 MeV and 15.11 MeV lines, no other background was necessary. This introduced an additional uncertainty in the relative yield of the 12.71 MeV gamma-ray due to uncertainty of the low energy tail of the line shape. To judge the effect of this uncertainty, the spectra were also fit with only the 12.71 MeV line and a variable quadratic background over a narrower channel region. The two fits agreed well: all structure was reproduced and the absolute yields overlapped, differing by a maximum of 5% on the high energy side ($E_p > 21$ MeV).

The yield curve of the 12.71 MeV gamma-ray duplicates quite well the recent results of Measday et al.,¹⁹ and Snover.⁴⁵ The peak at $E_p = 15.27$ MeV is identified as the $E_p = 15.22$ MeV peak seen in the elastic scattering and reaction data of Levine and Parker²⁰ ($E_x = 15.98$ MeV, $J^\pi = 7/2^+$, $\Gamma = 100$ keV). The peak at $E_p = 16.8$ MeV and corresponding dip at $E_p = 17.3$ MeV were previously seen by Snover. This structure can probably be accounted for by the two levels at $E_p = 16.5$ MeV ($E_x = 17.2$ MeV, $\Gamma = 500$ keV, seen in elastic and inelastic proton scattering

data by Daehnick and Sherr⁴⁶) and at $E_p = 17.27$ MeV ($E_x = 17.88$ MeV, $\Gamma = 400$ keV, seen by Snover et al.^{43,10}) interfering with a broad resonant background. The main strength which populates the 12.71 MeV level lies between 18 MeV and 22 MeV. With a bit of imagination, one can see a shoulder at $E_p = 18.8$ MeV, which coincides with a resonance seen by Daehnick and Sherr. One might also discern two separate peaks corresponding to resonances at $E_p = 19.4$ MeV ($E_x = 19.83$ MeV, $\Gamma = 1000$ keV, $J^\pi = 5/2^-$, $T = 1/2$, seen by Daehnick and Sherr and by Levine and Parker²⁰) and $E_p = 20.5$ MeV ($E_x = 20.9$ MeV, $\Gamma = 1500$ keV, $J^\pi = (5/2)^+$, seen in proton scattering by Scott et al.³⁰ and in the present 15.11 MeV gamma-ray yield, and that of Measday et al.¹⁹ The latter spin assignment has been questioned in section III, page 23, of this report.) Of course, these identifications are, at best, marginal. As in the yield of the 15.11 MeV gamma-ray, we again see the broad shoulder at $E_p = 22.4$ MeV.

Once again, the yield curve was fit in segments with pairs of Breit-Wigner shapes. Results are also given in table IV on page 47. The first two values given are the "weak" and "strong" interfering solutions. The third value, if given, is an estimate of the non-interfering strength. Either all the first or all the second values of solutions in brackets are self-consistent.

The peak at $E_p = 15.3$ MeV and the dip at $E_p = 17.3$ MeV were fit as resonances interfering with a broad resonant background. For the 15.3 MeV resonance, the strong solution seems unlikely.

The dip at 17.3 MeV was fit very well as an interfering resonance, but could not entirely account for the peak-shape near 16.7 MeV. This peak shape could include interference effects from the $E_p = 16.5$ MeV resonance ($E_x = 17.2$ MeV, $\Gamma = 500$ keV, seen by Daehnick and Sherr⁴⁶). The fitting program was not capable of handling three interfering resonances, but one might estimate the contribution of the 16.5 MeV resonance to be less than that of the 17.3 MeV resonance, that is $\Gamma_p < 50$ keV.

The resonances between 18 MeV and 24 MeV were fit with three non-interfering backgrounds subtracted: zero background, one-half the maximum possible background, and the maximum possible background = 13 ub/sr in this case. The proton widths quoted are for the fit which gave full widths in best agreement with accepted values, but the quoted errors include the uncertainty due to background subtraction.

Because the 12.71 MeV and 15.11 MeV states are so similar in structure, we can ask to what extent are they populated by the same compound nuclear states in ^{13}N ? Analogue states in ^{13}N ($T = 3/2$) would be isospin forbidden to decay to the 12.71 MeV ($T = 0$) state. However, analogue states must correspond to excited states in ^{13}B and ^{13}O . The resonances we are dealing with are far too broad to be identified with the low lying excited states of ^{13}B (no excited states of ^{13}O are known, at present). Thus, we assume that the compound nuclear states we are dealing with are $T = 1/2$ states. (Measday, Clegg and Fisher⁴⁹ argue that the broad ($\Gamma = 1000$ keV) state at $E_x = 26$ MeV

in ^{13}C and ^{13}N is the $T = 3/2$ component of the GDR, but this is at a significantly higher excitation energy.) Since transitions from these states to the 12.71 MeV level are not isospin suppressed, we shall consider those broad compound nuclear levels known to populate the 15.11 MeV level and those seen in proton scattering data to be primarily responsible for populating the 12.71 MeV state. To some extent, this is the best we can do, since the yield of the 12.71 MeV gamma-ray contains few well defined resonance shapes.

The small interfering solution for the 18.8 MeV resonance is consistent with the non-interfering estimate. The large solution seems unlikely in that it corresponds to a proton width of the 19.4 MeV resonance of 2300 keV, greater than the full width usually ascribed to that state ($\Gamma = 1500$ keV).

The fitting results show that interference effects could reduce the resonant contribution of the $E_p = 19.4$ MeV peak by an order of magnitude. If we identify this as the $J^\pi = 5/2^-$ state seen in proton scattering by Daehnick and Sherr⁴⁶ and by Levine and Parker,²⁰ and in agreement with its width, one would not expect to see interference effects with the positive parity state at $E_p = 20.5$ MeV in the ninety degree yield. In this case, the non-interfering estimate may well be more accurate. The same may be said of the $E_p = 22.4$ MeV resonance.

It should be emphasized that the 12.71 MeV gamma-ray yield from $E_p = 18$ MeV to 22 MeV can be fit equally well with a single broad resonant shape. The proton widths for the 18.8, 19.4, 20.5 and 22.4 MeV states should be considered an upper limit, at best.

C Angular Distributions of the 12.71 MeV
and 15.11 MeV Gamma-Rays

Angular distributions were taken at $E_p = 22.4$ MeV and 23.2 MeV, primarily to inspect structure in the $^{12}\text{C}(p,\gamma_0)$ yield. The yield was measured at five angles between 60° and 124° . Results for the capture and inelastic gamma-rays were given in section III A, figure 6 on page 27. In addition, the a_2 Legendre polynomial coefficient, defined by the equation

$$Y(\theta) = A_0 (1 + a_2 P_2(\cos\theta))$$

is given. The stated errors are those calculated in the error matrix (see appendix). Calculated angular distributions for this M1 radiation are given in table V on page 56.

The angular distribution of the 12.71 MeV gamma-ray remains constant at these energies. The value $a_2 = -0.34$ is seen to be consistent with a $p_{3/2}$ decay from a $J^\pi = 5/2^-$ level. At this energy, the 12.71 MeV gamma-ray sits on the tail of the 15.11 MeV gamma-ray. It should be noted that the gamma-ray resolution varies slightly with angle (resolution worsens for backward angles, where the spectrometer is very near the beam collimators). This is a small effect on the 15.11 MeV gamma-ray, but the errors on the 12.71 MeV gamma-ray value for a_2 have been increased to account for this inaccuracy.

The angular distribution of the 15.11 MeV gamma-ray changes dramatically, from being anisotropic at 22.4 MeV ($a_2 = -0.32 \pm .01$) to being very nearly isotropic at 23.3 MeV ($a_2 = -0.05 \pm .01$).

Table V

Angular distributions for $1^+ \rightarrow 0^+$ gamma-rays for the reaction $^{12}\text{C}(p,p'\gamma)$ where the intermediate radiation is unobserved.

J refers to the compound nuclear state. L_j refers to the unobserved proton.

J	L_j	Angular Distribution
1/2	$s_{1/2}-p_{1/2}-p_{3/2}$	P_0
3/2	$s_{1/2}-p_{1/2}$	$P_0 - 0.5 P_2$
	$d_{3/2}-p_{3/2}$	$P_0 + 0.4 P_2$
	$d_{5/2}-f_{5/2}$	$P_0 - 0.1 P_2$
5/2	$p_{3/2}-d_{3/2}$	$P_0 - 0.4 P_2$
	$f_{5/2}-d_{5/2}$	$P_0 + 0.46 P_2$
	$f_{7/2}-g_{7/2}$	$P_0 - 0.14 P_2$

Once again, the distribution at 22.4 MeV is consistent with a $5/2^-$ resonance. The distribution at 23.3 MeV, however, seems more consistent with either a $d_{5/2}$ transition from a $3/2$ state or an $s_{1/2}$ transition from a $1/2$ state, if populated primarily through a compound nuclear reaction. This mode of populating the 15.11 MeV state is implied by the proton scattering data of Scott et al.³⁰

The 55° yield for the 15.11 MeV and 12.71 MeV gamma-rays in this region was previously studied with this same spectrometer by Ebisawa et al.⁴⁷ This data for the 15.11 MeV gamma-ray was normalized to the present 90° yield, and the a_2 coefficient throughout this region was thus extracted. (This work was done by R. McDonald.⁴⁸) The results are shown in figure 13. The large error bars result from an uncertainty in the renormalization, which will hopefully be reduced by future measurements.

The value $a_2 = -0.5$ near 19.4 MeV agrees well with the assignment of $J^\pi = 3/2^+$ to that resonance. The decreased value of a_2 near 20.5 MeV only disallows the assignment $J = 1/2$. The value of a_2 is seen to become more negative past $E_p = 22$ MeV, which agrees with the a_2 value at 22.4 MeV from the present study.

V DISCUSSION

This study extends recent measurements, taken at the University of Washington, of the $^{12}\text{C}(p,\gamma_0)^{13}\text{N}$ reaction from $E_p = 2.8$ MeV to 24.4 MeV. The results have been re-normalized and are given in figure 14 on page 60. We estimate a 25 % uncertainty in the relative normalization of the different sets of data, and an equal uncertainty in the absolute yield. We hope to soon make measurements to better determine the relative normalizations.

Johnson has measured the γ_0 yield from $E_p = 2.8$ MeV to 9 MeV.¹⁹ He has shown, in particular, that the strong interference effect near $E_p = 5.3$ MeV can be explained by a coupled channel calculation which takes into account the contribution of the $J^\pi=2^+$ first excited state of ^{12}C to the ground state wave-function of ^{13}N . The work of Measday, Hasinoff and Johnson was described in section III B.

The most striking aspect of these results is the height of the giant resonance ($E_p = 20$ MeV) relative to the height of the pygmy ($E_p = 12$ MeV). The two peaks appear to contain equal strengths, making the terms "pygmy" and "giant" seem misnomers. The plotted results are differential cross-sections, and preliminary results indicate that variations in the angular distribution of the gamma-rays might enhance the yield near 20 MeV by as much as 25 %. Thus, with the uncertainty in relative normalizations,

DIFFERENTIAL CROSS-SECTION ($\mu\text{b}/\text{sr}$)

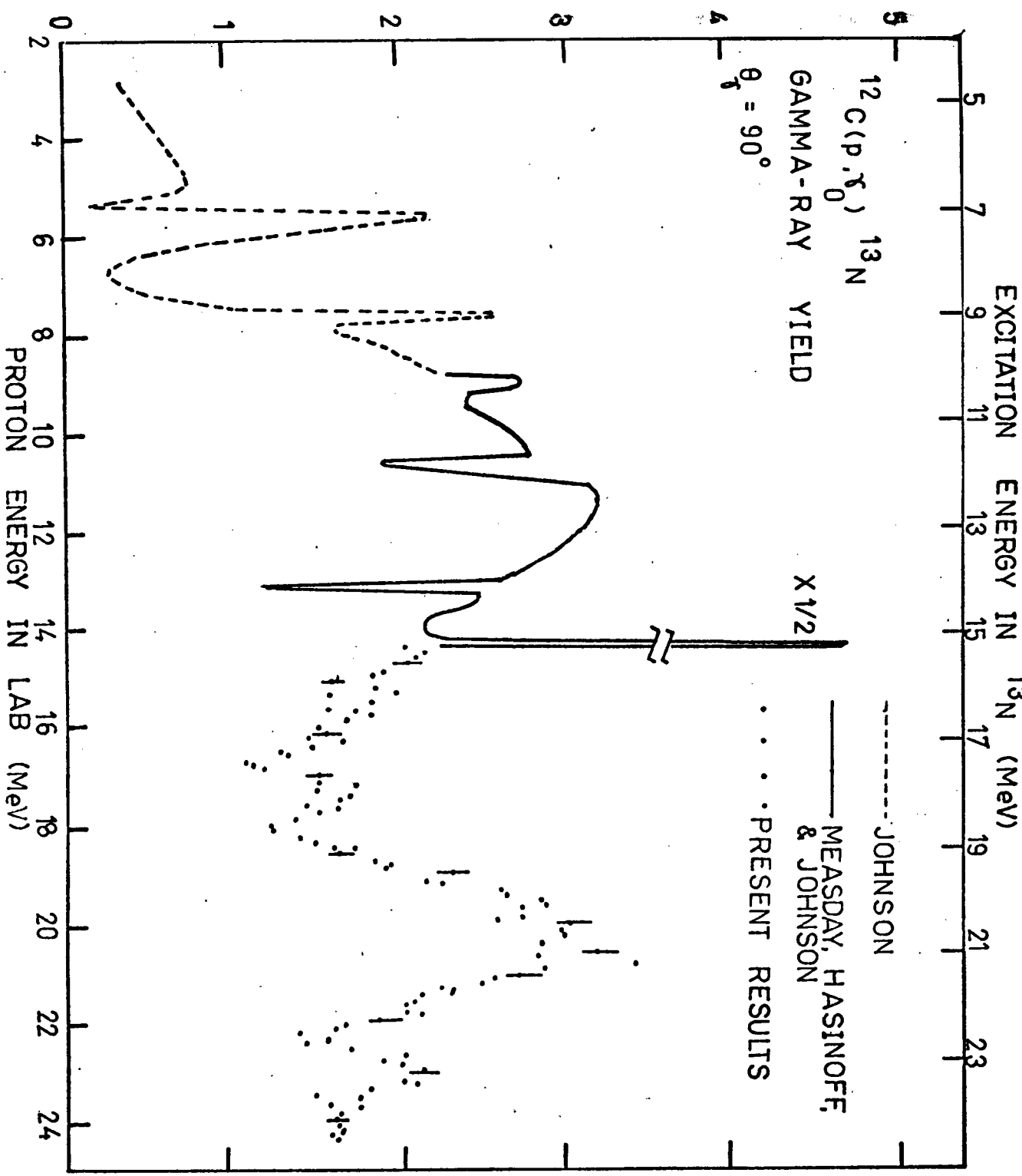


Figure 14

we can state only that the cross-section for the giant resonance cannot be greater than 150 % of the cross-section for the pygmy. Even considering the enhancement of low-energy yields by transitions to the ground state, mentioned in section I, this demands an abnormal amount of the dipole strength to be found at a very low energy for such a light nucleus.

The integrated cross-sections for the inverse reaction $^{13}\text{N}(\gamma, p_0)^{12}\text{C}$ calculated from this data are:

ΔE (MeV)	$\int \sigma dE$ (MeV-mb)
7 - 17	11
17 - 24.4	6

where the ratio of these numbers is uncertain by 40 %. These numbers are consistent with an earlier calculation by Measday et al.,⁴⁹ whose table we reproduce:

Values of $\int_0^E \sigma dE$ (MeV-mb) for photonuclear reactions

	Reaction	E (MeV)		
		17	23.5	32
from Measday et al. ⁴⁹	$^{13}\text{N}(\gamma, p_0)$	12	22	27
	$^{13}\text{C}(\gamma, n)$	21	55	109
	$^{13}\text{C}(\gamma, p)$	0	16	64

Measday's $^{13}\text{N}(\gamma, p_0)$ integrals include a contribution of ~ 0.9 MeV-mb from the 2.37 MeV first excited state of ^{13}N not included in our estimate. Even though our normalization is significantly lower than Measday's, our integrated cross section to 17 MeV is

essentially the same. In the present results, the pygmy resonance is seen to be broader than indicated by the earlier results used by Measday, which did not extend below $E_p = 10$ MeV. Measday's results for $^{13}\text{C}(\gamma, p)$ and $^{13}\text{C}(\gamma, n)$ are calculated from the data of Cook, 1957.¹¹

The $^{13}\text{N}(\gamma, p_0)^{12}\text{C}$ cross-section derived from a detailed balance calculation of the present results is given with the photo-disintegration data of Cook in figure 15, page 63, together with the theoretical calculations of Albert et al.²⁴ and Jager et al.⁵⁰ The curve labeled $^{13}\text{C}(\gamma, n) + ^{13}\text{C}(\gamma, pn) + ^{13}\text{C}(\gamma, 2n)$ was calculated from the experimental $^{13}\text{C}(\gamma, n) + ^{13}\text{C}(\gamma, pn) + 2\ ^{13}\text{C}(\gamma, 2n)$ results by taking a hypothetical $^{13}\text{C}(\gamma, 2n)$ cross-section and correcting for the double-counting of neutrons. This correction only affects the peak near $E_x = 26$ MeV, since the $(\gamma, 2n)$ threshold is 23.7 MeV. This correction has been criticized by Measday for ignoring the $^{13}\text{C}(\gamma, p')^{12}\text{B}^*$ decay to excited states in boron-12, which can further decay by neutron emission. Thus, Measday argues, the neutron decay cross-section could be lower at 26 MeV, and the proton decay cross-section higher. Easlea⁵¹ argues that the neutron decay cross-section should be higher at 26 MeV, on the basis of his schematic model calculation for ^{13}C using harmonic oscillator wavefunctions. Easlea's calculations show significant strength for dipole transitions in the region 10 - 17 MeV, but only after adding an ad-hoc interaction to correctly give the energy of the $J^\pi = 2^+$ excited state of ^{12}C at 4.43 MeV. This procedure has been

PHOTO-PRODUCTION CROSS-SECTIONS WITH THEORETICAL CALCULATIONS

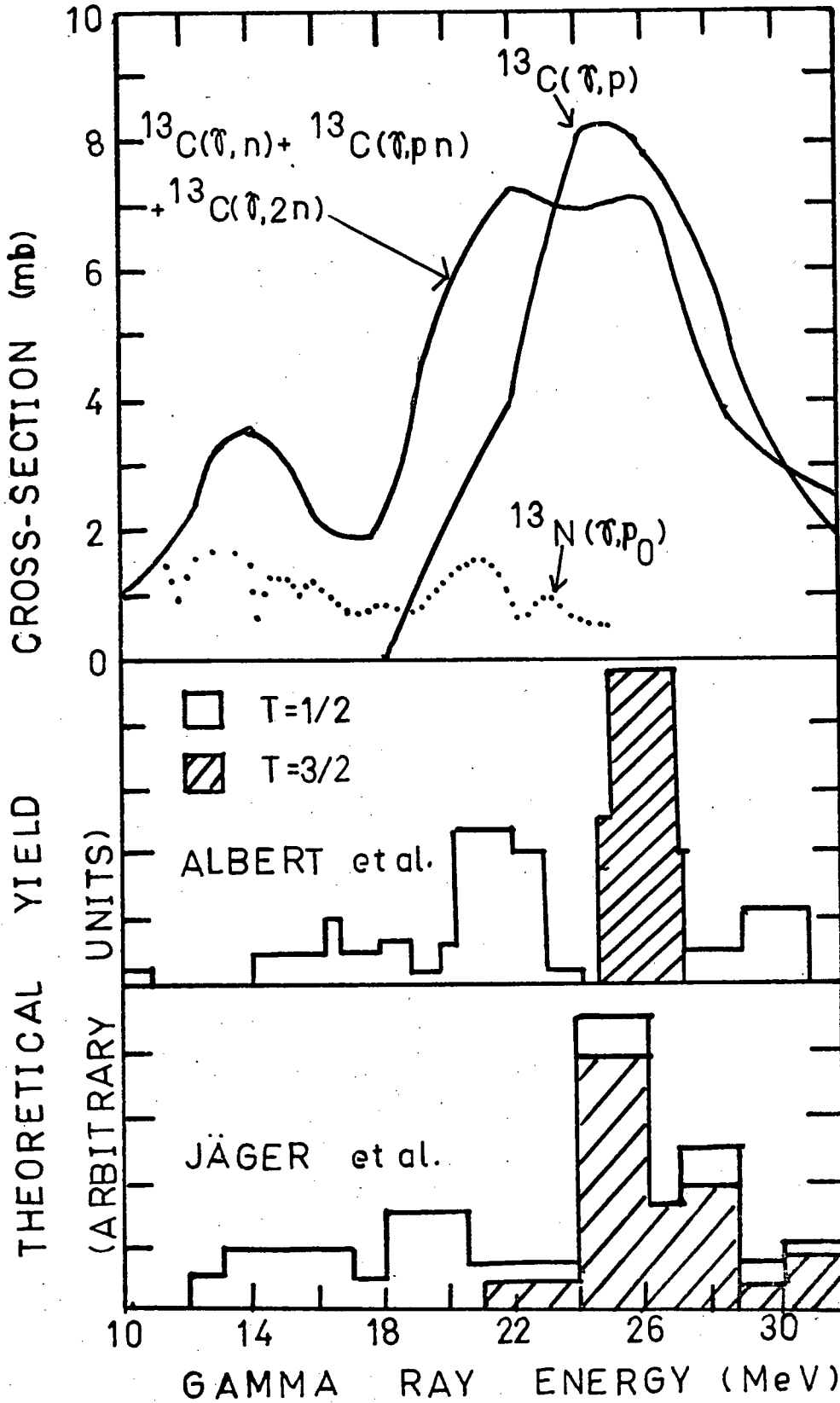


Figure 15

criticized by Measday and others. Figure 15 gives the results of a similar calculation by Albert et al.²⁴ with a more realistic Tabakin potential⁵² and no ad-hoc correction. This calculation shows some strength below 17 MeV, but does not adequately account for the pygmy resonance. The ¹³C calculations of Jager et al.,⁵⁰ using semi-phenomenological wave-functions, give better agreement with our results in the region of the pygmy resonance, at the expense of losing strength near the $E_x = 20$ MeV peak. Note that both calculations support Measday's argument that the 26 MeV resonance is an isospin $T = 3/2$ component of the giant resonance.

Jager gives a table of all shell model configurations contributing significantly to the dipole states in his model. The most important configurations (those contributing strength > 5 MeV-mb) are:

		(¹² C core)	(p _{3/2}) ⁻¹	(p _{1/2}) ¹	(d _{5/2}) ¹
from		"	(p _{3/2}) ⁻²	(p _{1/2}) ²	(d _{5/2}) ¹
Jager		"	(p _{3/2}) ⁻²	(p _{1/2}) ²	(2s) ¹
et al.	50	"	(p _{3/2}) ⁻³	(p _{1/2}) ³	(d _{5/2}) ¹

In the simple shell model picture, the ground states of ¹³C and ¹³N would be (¹²C core) (p_{1/2})¹, i.e. the valence nucleon.

We see that none of these configurations involve excitation of the valence nucleon. Only the first configuration, which carries most of the overall strength, is a lp-lh state. Excitation of (1s) nucleons contribute very little, and a configuration

(^{12}C core) $(d_{3/2})^1$, i.e. excitation of the valence nucleon, contributes only 0.05 MeV-mb at $E_x = 24.1$ MeV. Thus, Jager's calculation views the valence nucleon as a spectator, even in the region of the pygmy resonance. Transitions involving the valence nucleon should be seen most strongly in the inverse radiative-capture reaction, which leads us to speculate whether the peak seen at $E_p = 23$ MeV ($E_x = 23.2$ MeV) could be identified with Jager's $J^\pi, T = 3/2^+, 1/2$ state at $E_x = 24.1$ MeV.

To further support the view that the valence nucleon does not play an important role in dipole transitions to the ground state, we compare our measured cross-section for the $^{12}\text{C}(p, \gamma_0)^{13}\text{N}$ reaction to the cross-section for $^{11}\text{B}(p, \gamma_0)^{12}\text{C}$ measured by Allas et al.⁵³ in figure 16 on page 66. The excitation energy scales have been shifted by 2 MeV, but they have not been distorted. The excitation functions appear quite similar, containing three bumps in the region of the giant resonance. The energy shifts are:

	E_x (MeV)		
^{12}C	25.5	22.5	19.3
^{13}N	23.2	20.8	18.0
ΔE	2.3	1.7	1.3

The Q value for $^{12}\text{C} + p \rightarrow ^{13}\text{N}$ is + 2 MeV. We then see that, to correlate the peaks, we must shift the ^{12}C excitation energy scale by 4 MeV and stretch it by about 20 %. Since the excitation energies are determined by the shape of the potential well in

RADIATIVE PROTON CAPTURE YIELDS FOR ^{11}B AND ^{12}C

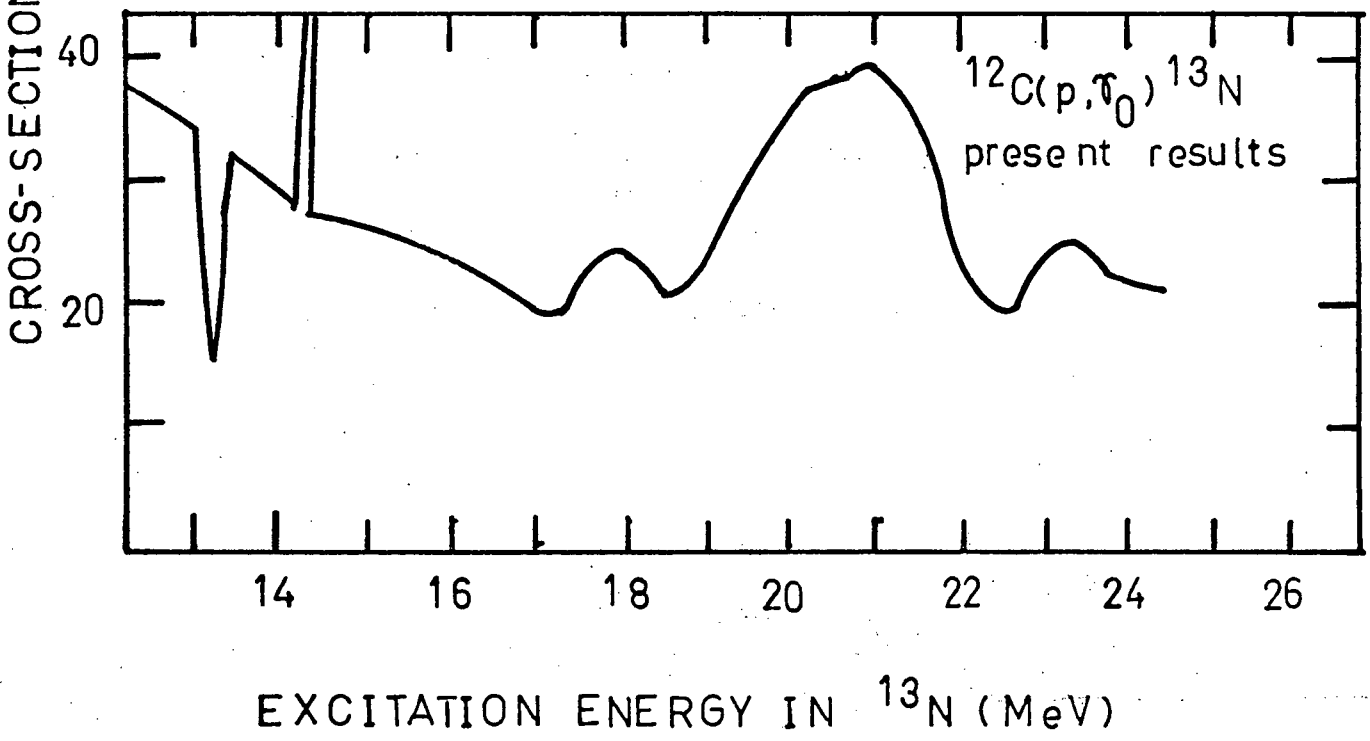
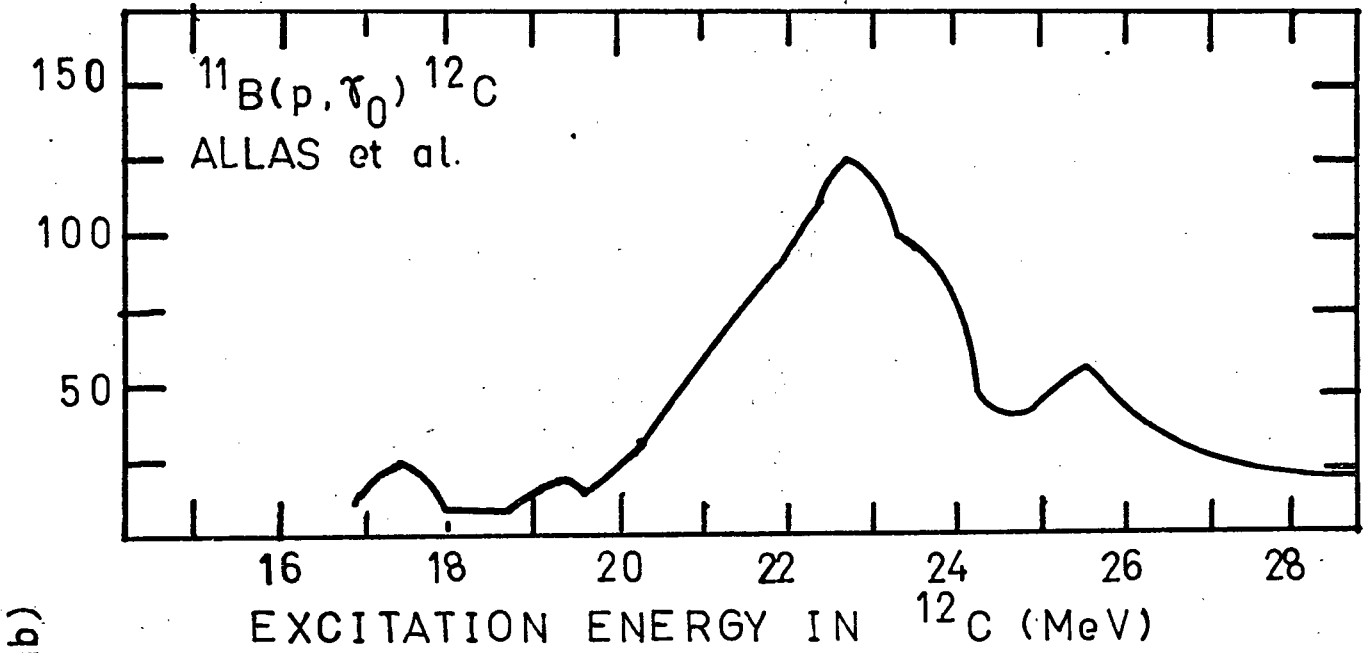


Figure 16

which the nucleons reside, which in turn arises from the sum total of nucleon-nucleon interactions, the distortion of the energy scale by the extra nucleon does not seem improbable.

The Q -value for $^{11}\text{B} + p \longrightarrow ^{12}\text{C}$ is + 15.96 MeV. The question arises whether the bump in the $^{11}\text{B}(p, \gamma_0)$ cross-section at $E_x = 17.5$ MeV could be related to the pygmy resonance in ^{13}N , but cut off by threshold effects. Were this the case, one might expect to see a bound state "pygmy" resonance in inelastic scattering reactions on ^{12}C . Bergstrom et al.⁵⁴ have done electroexcitation measurements on ^{13}C and ^{12}C . Bergstrom concludes that the addition of the valence neutron to the ^{12}C core causes a major restructuring of the giant resonance strength. This interpretation seems in conflict with the present results. However, Dixon, 1973,⁵⁵ has noted that the $^{12}\text{C}(\gamma, p)$ and $^{12}\text{C}(\gamma, p_0)$ cross-sections and angular distributions are significantly different, in localized regions. This discrepancy is caused by proton decays to excited states in ^{11}B . Similarly, we would argue that the re-distribution of dipole transition strength in ^{13}C compared to ^{12}C noted by Bergstrom is caused mainly by transitions to excited states in ^{12}C . Since most of these are transitions to the $J^\pi = 2^+$ state at $E_x = 4.4$ MeV, with a configuration (^{12}C core) $(p_{3/2})^{-1}(p_{1/2})^1$, the redistribution of strength for these transitions caused by the presence of a valence nucleon in the $p_{1/2}$ shell is not at all surprising.

Our results strongly support the view that valence nucleon transitions to the ground state from the GDR carry very little

strength in the region $E_x = 17 - 25$ MeV (and perhaps in the region $E_x = 7 - 17$ MeV).

In Bergstrom's data, the pygmy resonance (near $E_x = 14$ MeV) in ^{13}C is most visible in the form factor for electron energy and scattering angle $E_i = 106$ MeV, $\theta = 75^\circ$. In the corresponding ^{12}C data, a rather broad structure appears between $E_x = 9$ MeV and 13 MeV. We suggest that this may be the "analogue" of the pygmy resonance in mass-13 nuclei. This is, of course, only conjecture, and at present we cannot rule out the alternative interpretation that the pygmy resonance involves mainly valence nucleon transitions.

If the resemblance of the ^{11}B and ^{12}C radiative capture cross-sections is more than a coincidence, then the resonance at $E_x = 23.3$ MeV in ^{13}N should have a configuration identical to the $E_x = 25.5$ MeV resonance in ^{12}C with a spectator proton added. The comment of Brassard et al.⁹ that the 25.5 MeV resonance in ^{12}C is unexplained in the context of $1p-1h$ states is very interesting in this light.

A good deal of uncertainty exists concerning the possible resonance at $E_x = 23.2$ MeV in ^{13}N . A bump at this excitation energy was seen by Schiffer et al.⁵⁶ in $^{10}\text{B}(^3\text{He}, p)^{12}\text{C}^*$ proton decay at 0° . In the same reaction, Kuan et al., 1964,⁵⁷ found no anomaly. Simons et al., 1967,⁵⁸ found that, if a state exists, it does not have a strong effect on the polarization of the scattered proton. They note, however, that this is not entirely unlikely. A peak was seen by Patterson et al., 1966,⁵⁹ in the

150° yield proton decay to the ground state in ^{12}C . They speculate that it may be the broad 22.4 MeV level (see section IV) which comes at $E_{3\text{He}} = 0.5$ MeV, i.e. below the coulomb barrier. The resonance would be distorted by threshold effects, and their calculations support this possibility. In the $^{12}\text{C}(p,n)^{12}\text{N}(\beta^+)^{12}\text{C}$ reaction, Rimmer and Fisher, 1968,⁶⁰ find small peaks at $E_x = 21$ MeV and 23 MeV. In this reaction, the 22.4 MeV state should not be shifted. The calculation of Jager et al.⁵⁰ gives a state at 23.2 MeV, primarily of the configuration (^{12}C core) $(p_{3/2})^{-2}(p_{1/2})^2(2s)^1$. This state has $J^\pi = 3/2^+$. However, it has isospin $T = 3/2$, with no lp-lh configuration contributing. Some lp-lh strength would be necessary to see this state in a proton capture reaction. However, Jager also calculates a $J^\pi, T = 3/2^+, 1/2$ state should have $E_x = 24.1$ MeV. This state does have a significant lp-lh contribution, and so the 23.2 MeV state could be populated via some isospin mixing with the 24.1 MeV state.

Shakin and Wang⁶¹ have shown that including 3p-3h states in ^{16}O calculations quite successfully explain the intermediate structure in that GDR. Our results indicate that the 23 MeV resonance in ^{13}N may well be a 3p-2h state, and analogously, the 25.5 MeV state in ^{12}C might be either 3p-3h or 2p-2h. Although the present reasoning has been by no means rigorous, these conclusions remain an interesting possibility.

VI SUMMARY AND CONCLUSIONS

We have measured gamma-rays from the $^{12}\text{C}(p,\gamma)^{13}\text{N}$ reaction and from the inelastic reactions to the 12.71 MeV and 15.11 MeV states in ^{12}C for proton energies between 10 MeV and 24.4 MeV. Intermediate structure was found in the γ_0 yield in the region of the giant resonance. We note the similarity between this yield curve and that of the $^{11}\text{B}(p,\gamma_0)^{12}\text{C}$ yield. This has led us to speculate that the valence nucleon in nitrogen-13 is largely a spectator in the region of the GDR. This possibility is supported by the theoretical calculation of Jager et al., who used semi-phenomenological wave-functions. Jager's results indicate that the valence nucleon is a spectator even in the region of the pygmy resonance. Following this line of thought, we further speculate that the pygmy resonance in the mass-13 system may have a related "analogue" structure in carbon-12. We point out structure in electroexcitation data of carbon-12, measured by Bergstrom et al. that may correspond to this "bound state pygmy resonance".

Our measurements indicate that, for the (p,γ_0) reaction, the pygmy resonance carries strength approximately equal to the GDR. On the basis of angular distribution measurements, we verify the existence of two narrow minima super-imposed on the pygmy resonance, and agree in full with the suggestions

of Measday et al. concerning this structure.

We derive from our data yield curves for the 12.71 MeV and 15.11 MeV gamma-rays from the inelastic reaction, which agree well with other recent results. We list proton decay widths from compound nuclear states in ^{13}N to these states.

The (p, γ_1) and (p, γ_{2+3}) yields are also given for the regions in which they can be reliably extracted. No fine structure is seen.

The next step in determining the role of the valence nucleon in the mass-13 system might be to compare in detail angular distributions of the $^{11}\text{B}(p, \gamma_0)$ and $^{12}\text{C}(p, \gamma_0)$ reactions throughout the GDR. We hope to complete measurement of the latter quite soon. Extending recent measurements of the $^{11}\text{B}(d, \gamma_0) ^{13}\text{N}$ reaction beyond $E_x = 23$ MeV might also prove interesting. We further suggest that a theoretical calculation of the excitation energy distortion caused by the addition of a valence nucleon would prove valuable.

APPENDIX

The numerical results presented in this report were, for the most part, calculated using the following computer programs:

- 1) EGG - fits gamma-ray line shapes to a given spectrum
- 2) POLFT - fits a Legendre polynomial expansion to a given angular distribution.
- 3) INTER - fits interfering Breit-Wigner resonance shapes to a given yield curve.
- 4) FIND - locates approximately the second solution for INTER.

The first three programs were based almost entirely on the methods described in "Data Reduction and Error Analysis for the Physical Sciences" by Philip R. Bevington.²⁸ The author made only minor changes to each of these programs. The fourth was conceived and written by this author. A numerical program to apply efficiency corrections to the data and do a detailed balance calculation was also written, but is straightforward and will not be described.

A) EGG

The EGG program will fit up to ten gamma-rays to a given spectrum. The fitting routines are those described by Bevington. The program was adapted for use by M. Hasinoff and J. Spallone (who named it.)

The program first accepts two line shapes, creates up to 20 energy bins, and generates a line shape for each bin by linear interpolation. This allows the user to vary the resolution of the line shape with energy, or hold it fixed. EGG extrapolates the line shape to zero energy linearly to zero counts at zero energy, or with a horizontal slope, or with any slope in between, as instructed.

The program will fit up to ten gamma-rays simultaneously, and will vary positions and amplitudes as desired. The program will also add and vary a variety of backgrounds, including that described in section III. Another useful option allows the user to hold the excitation energy of any number of gamma-rays fixed with respect to the γ_0 .

The program varies the allowed parameters to minimize the reduced chi-squared, defined by:

$$\chi^2 = \frac{1}{\nu} \sum_i \left(\frac{(y_i - y(x_i))^2}{\sigma_i^2} \right)$$

where

σ_i^2 = the variance

y_i = data point at x_i

$y(x_i)$ = fit at x_i

ν = # of degrees of freedom

In order to minimize χ^2 , the program does a Taylor Series expansion:

$$\chi^2 = \chi_0^2 + \sum_j \left(\frac{\partial \chi_0^2}{\partial a_j} \delta a_j \right)$$

Using the method of least squares, the optimum values for the parameter increments are those for which

$$\frac{\partial \chi^2}{\partial a_k} = \frac{\partial \chi_0^2}{\partial a_k} + \sum_j \left(\frac{\partial^2 \chi_0^2}{\partial a_j \partial a_k} \delta a_j \right)$$

This results in simultaneous linear equations which can be solved as a matrix equation

$$\bar{\beta} = \bar{\delta a} \bar{\alpha} \quad (1)$$

where $\bar{\beta}$ and $\bar{\delta a}$ are row matrices and $\bar{\alpha}$ is a $r \times r$ square matrix.

$$\beta_k = - \frac{1}{2} \frac{\partial \chi_0^2}{\partial a_k}$$

$$\alpha_{jk} = \frac{1}{2} \frac{\partial^2 \chi_0^2}{\partial a_j \partial a_k}$$

Equation (1) is solved by matrix inversion, done in this case by rearrangement. The inverse of the curvature matrix $\bar{\alpha}$ is called the error matrix $\bar{\epsilon}$.

$$\bar{\epsilon} = \bar{\alpha}^{-1} \quad \text{or} \quad \bar{\alpha} \bar{\epsilon} = 1$$

The errors in the varied parameters determined by the error matrix ($\sigma_j^2 = \epsilon_{jj}$) includes both the statistical error and the uncertainty caused by relative uncertainties in the other varied parameters. Thus, the minimization is achieved by following the downward curvature of the χ^2 hyper-surface in a space having the varied parameters as co-ordinates.

The program has been adapted to produce plots of the fit and the data, which allows the user to see the quality of the fit. The program can fit a series of spectra from tape, or pick out individual spectra.

B) POLFT

The POLFT program can presently fit an angular distribution with Legendre polynomials up to fourth order. The input required is essentially the angles, yields and variances, together with the number of polynomials to be used and varied, and initial guesses for the coefficients. POLFT uses the same procedure for calculating errors and minimizing χ^2 as described in the previous section. It can also produce a plot of the data and the fit. The program has a wide range of options which were not used in this study.

C) INTER

This program, adapted by M. Hasinoff, uses the search technique described in section A. INTER fits a given excitation function with two interfering Breit-Wigner resonance shapes:

$$Y(E) = \left| S_A + S_G \right|^2$$
$$= \left| \frac{A_A}{\text{denA}} e^{i\phi} + \frac{A_G}{\text{denB}} \right|^2 \quad (2)$$

$$\begin{aligned}
 &= \left| \frac{A_A}{\text{denA}} \right|^2 + \left| \frac{A_G}{\text{denB}} \right|^2 + \frac{A_A A_G}{(\text{denA denB})^2} \\
 &\quad \times \left[2 \cos \varphi \left\{ (E-E_A)(E-E_G) + \frac{\Gamma_A \Gamma_G}{4} \right\} \right. \\
 &\quad \left. - 2 \sin \varphi \left\{ \frac{\Gamma_A}{2} (E-E_G) - \frac{\Gamma_G}{2} (E-E_A) \right\} \right]
 \end{aligned}$$

where

$$\begin{aligned}
 A_A &= \text{strength of resonance A} \\
 &= (\pi \lambda^2 \Gamma_A^{\text{in}} \Gamma_A^{\text{out}})^{\frac{1}{2}}
 \end{aligned}$$

$$E_A = \text{energy of resonance A}$$

$$\Gamma_A = \text{full width of resonance A}$$

$$\varphi = \text{relative phase between the resonances}$$

$$\Gamma_A^{\text{in}} = \text{width of incoming channel of resonance A}$$

$$\Gamma_A^{\text{out}} = \text{width of outgoing channel of resonance A}$$

$$\text{denA} = E - E_A + i \frac{\Gamma_A}{2}$$

and similarly for resonance G.

The program is capable of varying the strength, width, and centroid energy of each resonance, and the relative phase, as desired. The program follows the χ^2 minimizing procedure described in section A, and produces plots of the data and the fit.

An excitation function with two peaks can frequently be fit with two entirely separate sets of parameters. This is further described in the following section.

D) FIND

Fitting two interfering Breit-Wigner resonance shapes to a yield curve frequently results in two sets of solutions. This type of fitting was first done for the case of a narrow ($T_{>}$) analogue state interfering with a broad ($T_{<}$) state, and the two solutions have been called the "strong" solution, corresponding to a strong analogue state interfering with a weak background (the $T_{<}$ state), and the "weak" solution, i.e. a weak analogue state interfering with a strong background. Thus, the two solutions are characterized by very different ratios for A_A/A_G , and usually a variation in the relative phase. For this type of interference, the weak solution has usually been determined to be the physical solution by comparing results to other available information about the resonance.

We present a simplified picture to explain the origin of two solutions, and to locate the "other" solution after one has been found. First, we picture the two Breit-Wigner shapes as vectors in the complex plane. Then

$$Y(E) = \left| \bar{S}_A e^{i\varphi} + \bar{S}_G \right|^2$$

where the vectors are obviously derived from equation (2).

The vectors are, of course, energy dependent. In particular

$$\begin{aligned}
 Y(E_G) &= \left| \frac{A_A}{\Delta E - i\frac{\Gamma_A}{2}} e^{i\varphi} + \frac{A_G}{-i\frac{\Gamma_G}{2}} \right|^2 \\
 &= \left| \bar{S}_A^{-1} e^{i\varphi} + \bar{S}_G^{-1} \right|^2 \quad (3)
 \end{aligned}$$

with $\Delta E = (E_G - E_A)$

The angle φ is not actually the angle between the vectors because the vectors themselves contain imaginary factors.

In fact, \bar{S}_G^{-1} is oriented along the imaginary axis, and for $\varphi = 0$, \bar{S}_A^{-1} points at an angle β^1 where

$$\beta^1 = \arccos \frac{\Delta E}{\text{den}A_1} = -\arcsin \frac{\Gamma_A/2}{\text{den}A_1}$$

where $\text{den}A_1 = \Delta E + i\Gamma_A/2$. Then \bar{S}_A^{-1} is in the fourth quadrant for ΔE positive, and the third quadrant for ΔE negative.

φ is then the angle which vector \bar{S}_A^{-1} is rotated from this initial position. We re-normalize equation (3) such that vector \bar{S}_A^{-1} has the norm A_A . We see, then, that for a given yield and a given strength for resonance G, a strength for resonance A can be found for any phase angle φ at this energy. The vector \bar{S}_A^{-1} traces out an ellipse as φ is varied through 2π . This situation is depicted by the solid lines in figure 17 (a). Of course a good solution must hold for the yield at all energies. We now look at the corresponding equation for the yield at

GEOMETRIC MODEL FOR DOUBLE SOLUTIONS TO INTERFERING BREIT-WIGNER RESONANCE SHAPES

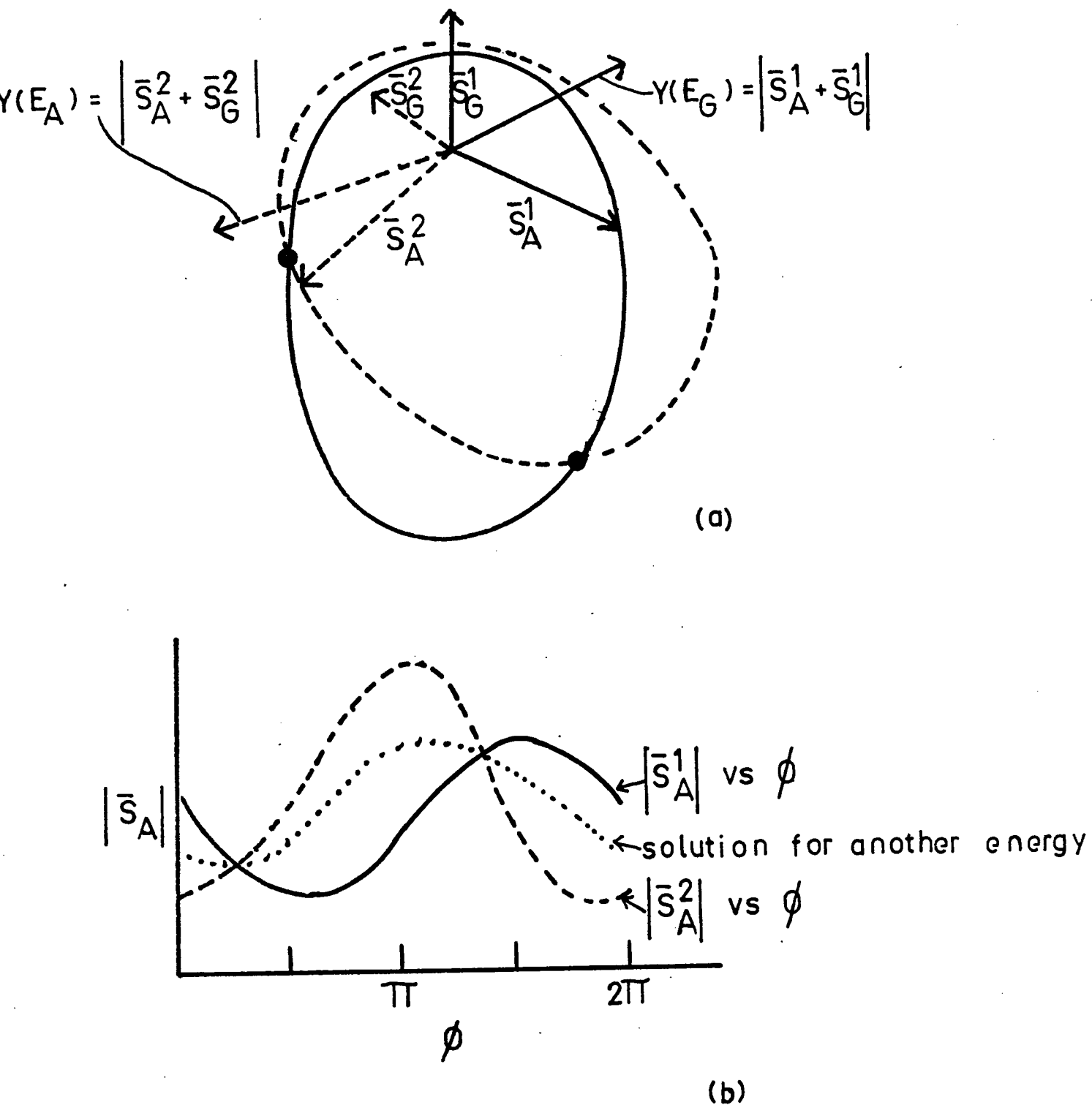


Figure 17

energy E_A . The situation is similar, but vector \bar{S}_G^2 does not point along the imaginary axis and the vector \bar{S}_A^2 points in a different direction for $\varphi = 0$. To determine a solution good at both energies, we must rotate this system so that \bar{S}_A^2 overlays \bar{S}_A^1 at $\varphi = 0$ and also re-normalize $|\bar{S}_A^2| = A_A$. Again we can determine a solution for \bar{S}_A^2 for any value of φ , and the locus of solutions traces a second ellipse. These are the dashed lines in figure 17 (a). We see that the two ellipses will usually intersect at two points, corresponding to two solutions for the relative phase φ and the strength A_A , for the same strength A_G .

Of course, for both solutions to be good solutions they must hold at all energies, i.e. many ellipses must pass through these two points. In figure 17 (b), we plot strength A_A versus φ for the two energies E_G and E_A and for an arbitrary energy. Since the solution for S_A must be periodic in φ (period = 2π) for any energy, the solutions for S_A must cross twice if they cross at all. They can be non-intersecting or tangent. However, if one pair of ellipses intersect for a given yield, it seems plausible that ellipses will intersect for all energies.

A simple program was written making use of this picture. For the two resonant energies, solutions for the strength of one resonance was calculated for values of φ between 0 and 2π , holding the strength of the other resonance fixed at the value of the first solution found by INTER. The second solution,

LEAF 81 OMITTED IN PAGE NUMBERING.

where the strengths of A_A are equal for a given φ , was found by inspection. These new guesses for A_A and φ were then supplied to the INTER program.

The program FIND successfully located the other solution approximately 75 % of the time. Some of the difficulties are thought to arise from the simplified assumptions made, i.e. that the values of A_G , Γ_A , Γ_G , E_A , and E_G remain unchanged in the physical situation. The program is being subject to further tests.

bibliography:

- 1 Brink, D.M., 1957, Nuc. Phys. 4, 215
- 2 Goldhaber, M., and E. Teller, 1948, Phys. Rev. 74, 1046
- 3 Danos, M., 1973, Asilomar Int. Conf. on Photo-nuclear
Reactions and Applications, p. 43
- 4 Danos, M., and E. G. Fuller, 1965, Ann. Rev. of Nuc. Sci.,
15, 29 (see page 52)
- 5 Wilkinson, D.H., 1956, Physica 22, 1039
- 6 Allas, R.G., S.S. Hanna, L. Meyer-Schutzmeister, R.E. Segel,
P.P. Singh, Z. vager, 1964, Phys. Rev. Lett. 13, 628
- 7 Tanner, N.W., 1965, Nuc. Phys. 63, 383
- 8 Brown, G.E., and M. Bolsterli, 1959, Phys. Rev. Lett. 3, 472
- 9 Brassard, C., H.P. Shay, J.P. Coffin, W. Scholz, and
D.A. Bromley, 1972, Phys. Rev. C6, 53
- 10 Ajzenberg-Selove, F., 1970, Nuc. Phys. A152, 1
- 11 Cook, B.C., 1957, Phys. Rev. 106, 300
- 12 Von Butlar, H., 1968, Introduction to Nuclear Physics,
Academic Press, N.Y., N.Y.
- 13 Henley, E.M., 1969, Ann. Rev. of Nuc. Sci. 19, 367
- 14 Segel, R.E., Asilomar Int. Conf. on Photo-nuclear Reactions
and Applications, p. 899
- 15 Warburton, E.K., and H.O. Funsten, 1962, Phys. Rev. 128, 1810
- 16 Fisher, P.S., D.F. Measday, F.A. Nikolaev, A. Kalmykov,
and A.B. Clegg, 1963, Nuc. Phys. 45, 113

- 17 Dietrick, F.S., M. Suffert, A.V. Nero, S.S. Hanna, 1968
Phys. Rev. 168, 1169
- 18 Johnson, D.L., 1974, Doctoral thesis, University of Washington
(unpublished)
- 19 Measday, D.F., M. Hasinoff, D.L. Johnson, 1973, Can. J.
of Phys., 51, 1227
- 20 Levine, M.J., and P.D. Parker, 1969, Phys. Rev. 186, 1021
- 21 Meyer, H.O., and G.R. Plattner, 1973, Nuc. Phys. A199, 413
- 22 Rimmer, E.M., and P.S. Fisher, 1968, Nuc. Phys. A108, 561,567
- 23 Motz, H.T., Ann. Rev. of Nucl. Sci., 20, 1
- 24 Albert, D.J., R.F. Wagner, H. Uberall, and C. Werntz,
1969, High Energy Phys. and Nucl. Structure, Ed. Devons, p. 89
- 25 Hasinoff, M.D., S.T. Lim, D.F. Measday, T.J. Mulligan,
1974, Nucl. Inst. and Methods, to be published
—— Ann. Report, Nucl. Phys. Lab., U. of Wash., p. 19
- 26 Lim. S.T., 1974, Doctoral thesis, University of B.C.
- 27 Photon Cross Section Attenuation Coefficients and
Energy Coefficients from 10 keV to 100 GeV, U.S.
Dept. of Commerce, NSRDS, NBS#29, Aug. 1969
- 28 Bevington, P.R., Data Reduction and Error Analysis for
the Physical Sciences, 1969, McGraw-Hill, N.Y., N.Y.
- 29 Lowe, J., and D.L. Watson, 1966, Phys. Lett., 23, 261
Erratum: 24B, 174
- 30 Scott, D.K., P.S. Fisher, and N.S. Chant, 1967, Nuc. Phys.
A199, 177

- 31 Szucs, J., J.E. Cairns, N.W. Greene, J.A. Kuehner, 1973
Physics in Canada 29, 4
- 32 Adelberger, E.G., A.B. McDonald, C.L. Cocke, C.N. Davids,
A.P. Shukla, H.B. Mak, D. Ashery, 1973, Phys. Rev. C7, 889
- 33 Wilkinson, D.H., 1959, Ann. Rev. of Nuc. Phys. 1,1
- 34 Adams, H.S., J.D. Fox, N.P. Heydenburg, and G.M. Temmer,
1961, Phys. Rev. 124, 1899
- 35 Ajzenberg-Selove, F. and T. Lauritsen, 1968, Nucl. Phys.
A114, 1
- 36 Cecil, F.E., L.W. Fagg, W.L. Bendel, E.C. Jones, 1974,
Phys. Rev. C9, 798
- 37 Riesman, F.D., P.I. Connors, and J.B. Marion, 1970,
Nucl. Phys. A153, 244
- 38 Adelberger, E.G., and J.E. Bussoletti, 1973, Ann. Report,
Nuc. Phys. Lab., U. of Wash., p. 30
- 39 Chertok, B.T., C. Sheffield, S.W. Lightbody, S. Penner,
and D. Blum, Phys Rev C8, 23
- 40 Alburger, D.E., and D.H. Wilkinson, 1972, Phys Rev, C5, 384
- 41 Braithwaite, W.J., J.E. Bussoletti, F.E. Cecil, and
G.T. Garvey, 1972, Phys. Rev. Lett. 29, 276
- 42 Ebisawa, K., M.D. Hasinoff, D.L. Johnson, S.T. Lim and
K.A. Snover, 1973, Ann. Report, Nuc. Phys. Lab., U. of
Wash., p. 102

- 43 Snover, K.A., E.G. Adelberger, and Reiss, 1968, Bull. Am. Phys. Soc. 13, 1662
- 44 Measday, D.F., P.S. Fisher, A. Kalmykov, F.A. Nikolaev, and A.B. Clegg, 1963, Nuc. Phys. 45, 98
- 45 Snover, K.A., 1973, private communication
- 46 Daehnick, W.W. and R. Sherr., 1964, Phys. Rev. 133, B934
- 47 Ebisawa, K., M. Hasinoff, S.T. Lim, D.F. Measday, T.J. Mulligan, and J.E. Spuller, 1973, Ann. Report, Nuc. Phys. Lab., U. of Wash., p. 100
- 48 McDonald, R., 1974, private communication
- 49 Measday, D.F., A.B. Clegg, P.S. Fisher, 1965, Nuc. Phys. 61, 269
- 50 Jager, H.U., H.R. Kissener, R.A. Eramzhian, 1971, Nuc. Phys. A171, 16
- 51 Easlea, B.R., 1962, Phys. Lett. 1, 163
- 52 Tabakin, F., 1964, Ann. Phys. 30, 51
- 53 Allas, R.G., S.S. Hanna, L. Meyer-Schutzmeister, R.E. Segel, 1964, Nuc. Phys. 58, 122
- 54 Bergstrom, J.C., H. Crannel, F.J. Kline, J.T. O'Brien, J.W. Lightbody Jr., and S.P. Fivozinsky, 1971, Phys. Rev. C4, 1514
- 55 Dixon, J., 1973, Asilomar Int. Conf. on Photo-nuclear Reactions and Applications, p. 727

- 56 Schiffer, J.P., T.W. Bonner, R.H. Davis, and F.W. Prosser Jr.,
1956, Phys. Rev. 104, 1064
- 57 Kuan, H., P.R. Almond, G.U. Din, and T.W. Bonner, 1964,
Nuc. Phys. 60, 509
- 58 Simons, D.G., 1967, Phys. Rev. 155, 1132
- 59 Patterson, J.R., J.M. Poate, and E.W. Titterton, 1966,
Proc. Phys. Soc. 88, 641
- 60 Rimmer, E.M., and P.S. Fisher, 1968, Nuc. Phys. A108, 561
- 61 Shakin, D.M., and W.L. Wang, 1971, Phys. Rev. Lett. 26, 902